nature food

ARTICLES

https://doi.org/10.1038/s43016-022-00530-x

Check for updates

OPEN

A hybrid inorganic–biological artificial photosynthesis system for energy-efficient food production

Elizabeth C. Hann[1,2,5], Sean Overa[3,5], Marcus Harland-Dunaway[1,2,5], Andrés F. Narvaez[1,4], Dang N. Le[1], Martha L. Orozco-Cárdenas[4], Feng Jiao[3] ✉ and Robert E. Jinkerson[1,2] ✉

Artificial photosynthesis systems are proposed as an efficient alternative route to capture CO_2 to produce additional food for growing global demand. Here a two-step CO_2 electrolyser system was developed to produce a highly concentrated acetate stream with a 57% carbon selectivity (CO_2 to acetate), allowing its direct use for the heterotrophic cultivation of yeast, mushroom-producing fungus and a photosynthetic green alga, in the dark without inputs from biological photosynthesis. An evaluation of nine crop plants found that carbon from exogenously supplied acetate incorporates into biomass through major metabolic pathways. Coupling this approach to existing photovoltaic systems could increase solar-to-food energy conversion efficiency by about fourfold over biological photosynthesis, reducing the solar footprint required. This technology allows for a reimagination of how food can be produced in controlled environments.

Food demand is growing globally, but food production is ultimately constrained by the energy conversion efficiency of photosynthesis. Most crop plants can convert sunlight and CO_2 into plant biomass at an energy conversion efficiency of only ~1% or less[1]. Large tracts of land are thus required for crop cultivation to capture the requisite solar energy to provide food for humanity. Recent breeding and genetic engineering efforts to increase photosynthetic efficiency have yielded only select gains in a limited number of food crops[2–4]. Increasing the energy efficiency of food production (solar-to-biomass conversion) would allow for more food to be produced using less resources.

Artificial photosynthesis seeks to overcome the limitations of biological photosynthesis, including low efficiency of solar energy capture and poor carbon dioxide reduction, and could provide an alternative route for food production. Recent studies have demonstrated systems that convert CO_2 and H_2O into reduced species, such as CO, formate, methanol and H_2, through electrolysis processes. CO_2, CO and H_2 can be upgraded to fuels and chemicals through gas-phase fermentation by select bacteria[5–7]; however, gas–liquid mass transfer limits the volumetric efficiency and results in uneconomic fermentation systems. The use of formate or methanol as a carbon source for fermentation is limited because formaldehyde, a toxic intermediate, is formed during biological metabolism of these substrates[8–10]. To date, electrochemically derived substrates cannot support the growth of most food-producing organisms[11]. However, acetate is a soluble, two-carbon substrate that can be electrochemically produced[12] and is more readily metabolized by a broad range of organisms. The use of acetate produced from CO_2 electrolysis to cultivate food-producing organisms could allow food production independent of biological photosynthesis but has not yet been demonstrated.

Here we describe the development of a hybrid inorganic–biological system for food production. A two-step electrochemical process converts CO_2 to acetate, which serves as a carbon and energy source for algae, yeast, mushroom-producing fungus, lettuce, rice, cowpea, green pea, canola, tomato, pepper, tobacco and *Arabidopsis* (*A. thaliana*) (Fig. 1). Coupling this system of carbon fixation to photovoltaics offers an alternative, more energy-efficient approach to food production.

Results

Acetate production from CO_2 electrolysis. To provide a carbon and energy source independent of biological photosynthesis that can sustain the growth of food-producing organisms, we developed an electrocatalytic process to produce acetate (as either sodium or potassium acetate depending on the electrolyte salt) from CO_2. Acetate produced directly from electrochemical CO_2 reduction using a copper catalyst has a less than 15% carbon selectivity, which is defined as the amount of carbon in the end product(s) divided by the total amount of carbon reduced in the system[13–16]. However, recent studies on CO reduction have demonstrated that acetate can be produced at industrially relevant reaction rates with a carbon selectivity of greater than 50% using a nanostructured copper catalyst[12,17,18]. To achieve maximum selectivity and production of acetate from a direct CO_2 feed, a two-step electrolyser system was demonstrated to convert CO_2 to CO and then CO to acetate through a tandem process (Fig. 2a and Extended Data Fig. 1a). More specifically, CO_2 is fed to the cathode of the first electrolyser, which utilizes a commercial silver catalyst supported on a gas diffusion layer (that is, a carbon paper) and produces a gaseous product stream containing CO, H_2 and trace CO_2. The gas diffusion electrode improves the gaseous CO_2 transport to the electrocatalyst, achieving higher

[1]Center for Industrial Biotechnology, Department of Chemical and Environmental Engineering, University of California, Riverside, CA, USA. [2]Center for Plant Cell Biology, Department of Botany and Plant Sciences, University of California, Riverside, CA, USA. [3]Center for Catalytic Science and Technology, Department of Chemical and Biomolecular Engineering, University of Delaware, Newark, DE, USA. [4]Plant Transformation Research Center, University of California, Riverside, CA, USA. [5]These authors contributed equally: Elizabeth C. Hann, Sean Overa, Marcus Harland-Dunaway. ✉e-mail: jiao@udel.edu; robert.jinkerson@ucr.edu

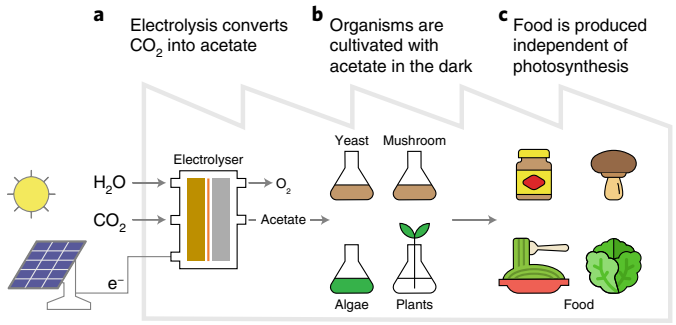

Fig. 1 | A combined electrochemical–biological system for the production of food from CO_2. **a**, CO_2 electrolysis uses electricity (generated by photovoltaics) to convert CO_2 and H_2O into O_2 and acetate. This process was optimized to produce an effluent output ideal for supporting the growth of food-producing organisms. **b**, *Chlamydomonas*, *Saccharomyces*, mushroom-producing fungus and a variety of vascular crop plants were grown using the electrolyser-produced effluent. **c**, The organisms grown using the electrolyser-produced effluent serve as food or food products. This system is capable of making food independent of photosynthesis, using CO_2, H_2O and solar energy.

currents towards CO_2 reduction products compared with dissolved CO_2 in a typical batch reactor[16,19–21]. A solution of 1 M $KHCO_3$ in deionized water was used as the electrolyte on the anode side (that is, anolyte) for the CO_2 electrolyser and recirculated through the anode compartment to maintain the ionic conductivity. The presence of an aqueous electrolyte has been shown to reduce the total cell potential for anion exchange membrane-based CO_2 electrolysers[13,22]. An IrO_2 anode was utilized for CO_2 reduction, due to its stability in neutral pH. The gas product stream was then fed to the cathode chamber of the CO electrolyser, which contains a commercial copper catalyst for CO reduction, 1 M KOH as the anolyte and a $NiFeO_x$ anode. This design is similar to a tandem system previously reported by Romero Cuellar et al.[23]. By maximizing the conversion of the first and second electrolysers, as well as specifically targeting acetate over other multi-carbon products, this system was able to achieve a single-pass conversion of CO_2 to acetate of 25%, a large improvement over the <1% conversion previously reported (Supplementary Table 1). Effluents, the liquid products of electrolysis containing acetate and other by-products (Extended Data Fig. 1c,d), were evaluated as carbon and energy sources for the cultivation of food-producing organisms. Early experiments found that effluents with an acetate-to-electrolyte ratio below 0.4 did not support the growth of algae (Supplementary Note). Maximizing the ratio of acetate to electrolyte was therefore crucial for integrating these carbon products with biological food production.

Operating parameters of the tandem CO_2 electrolysis system were identified that maximized the conversion of CO_2 feed to acetate. For the production of CO, the operating current density of the CO_2 electrolyser was 100 mA cm^{-2} at an inlet flow rate of 7 ml min^{-1} CO_2, which maximized CO_2 conversion to CO at 43% and maintained a high level of performance (Extended Data Fig. 1e–h).

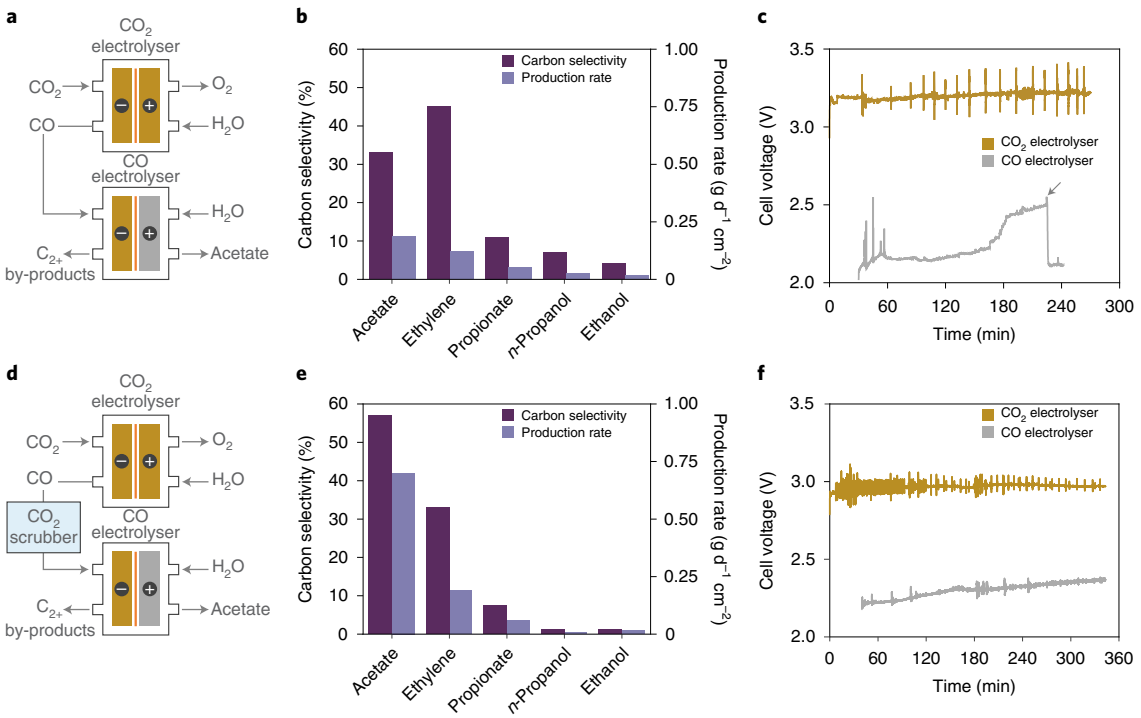

Fig. 2 | A two-step electrochemical process can reduce CO_2 to acetate with high carbon selectivity. a–f, Early (**a**–**c**) and optimized (**d**–**f**) two-step electrolysis systems for the production of acetate. Panels **a** and **d** show overviews of the schematics. Effluent containing acetate is collected in the anode compartment of the CO electrolyser. In **b** and **e**, carbon selectivities towards specific products and area-normalized production rates are shown. Acetate, propionate, *n*-propanol and ethanol were collected and quantified in effluent, ethylene was quantified continuously over the course of the experiment and the average value is presented. In **c** and **f**, the electrolyser voltage stabilities of CO_2 electrolyser (gold) and CO electrolyser (silver) are shown. CO_2 electrolyser operated for the entire experiment using 1 M $KHCO_3$ electrolyte, a silver nanoparticle cathode and an iridium oxide anode. CO electrolyser operation began after 30 minutes using 1 M KOH electrolyte, a copper nanoparticle cathode and a nickel iron oxide anode. CO_2 flow was held constant at 7 ml min^{-1}. Oscillations in potential were caused by fluctuations in the back-pressure controller. Panel **c** shows a voltage increase over the time observed. Fresh KOH was fed to recover the electrolyser voltage (arrow) to determine whether the electrolyser voltage increase was due to the acidification of electrolyte. The CO_2 scrubber contained 5 M NaOH to capture residual CO_2.

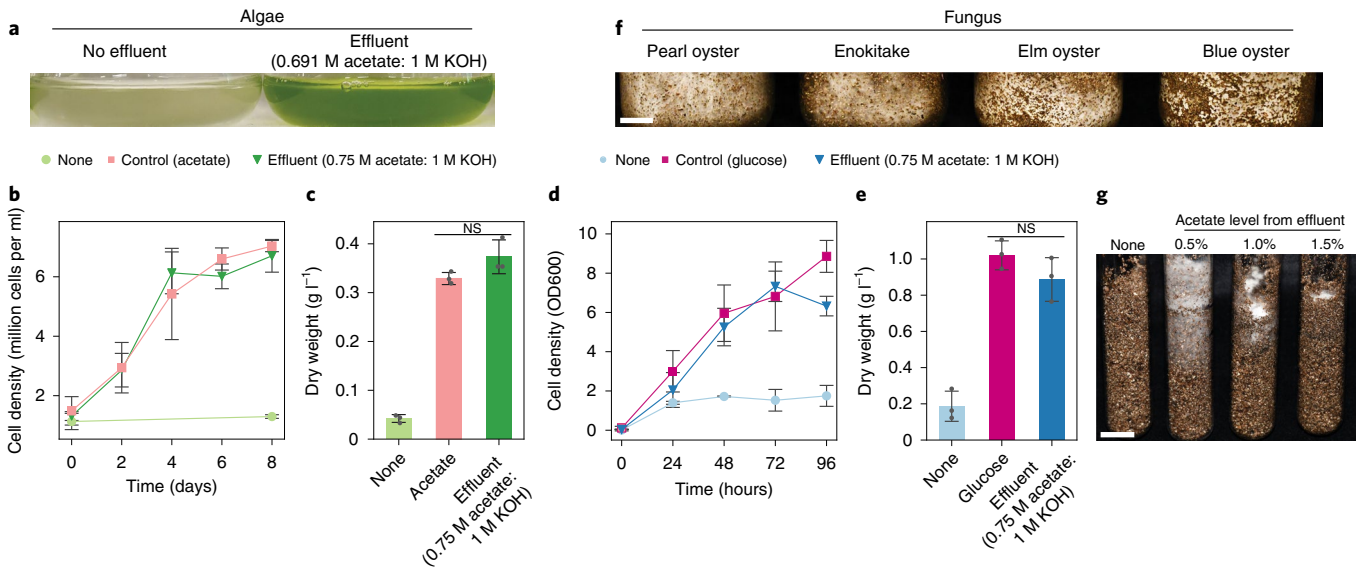

Fig. 3 | *Chlamydomonas*, *Saccharomyces* and mushroom-producing fungus can grow heterotrophically with effluent as the sole carbon and energy source. a, Image of *Chlamydomonas* cultures taken after four days of growth in darkness; the cultures were grown with effluent (0.691 M acetate: 1 M KOH) or with no effluent. **b**,**c**, Growth of *Chlamydomonas* cultures grown in the dark, shaking, at 30 °C, with effluent (0.75 M acetate: 1 M KOH), with acetate (control) or with neither (no acetate or effluent). Panel **b** shows daily cell counts for eight days of growth, and **c** shows dry weight after two days of growth. *Chlamydomonas* cultures were grown in TAP media with acetate, without acetate or with effluent in place of acetate to match the acetate concentration of a typical liquid heterotrophic growth medium (17.5 mM). All *Chlamydomonas* media were adjusted to pH 7.2. **d**,**e**, *Saccharomyces cerevisiae* cultures were grown at 30 °C, shaking, in YPD media with glucose (3.45 g l^{-1}), without glucose (0 g l^{-1}) or with effluent (0.75 M acetate: 1 M KOH) in place of glucose with an acetate concentration to match the energetic equivalent of 3.45 g glucose per l (53.36 kJ l^{-1}). All *Saccharomyces* media were adjusted to pH 6.0. Panel **d** shows optical density (OD) (600 nm) over 96 hours. Panel **e** shows dry weight 24 hours after inoculation. In **b**–**e**, each data point represents three biological replicates. The error bars represent standard deviations. In **c** and **e**, two-tailed unpaired *t*-tests showed no significant difference between *Chlamydomonas* growth in acetate and in effluent media ($P = 0.1045$) and no significant difference between *Saccharomyces* growth in glucose and in effluent media ($P = 0.1857$). NS, not significant. **f**, Images of pearl oyster, enokitake, elm oyster and blue oyster mushroom mycelium from colonization of a solid vermiculite substrate soaked with YPD media containing simulated effluent in place of glucose (0.0691 M acetate: 1 M KOH) to reach 0.5% (w/w) acetate as the primary carbon and energy source. The images were taken 24 days after inoculation. Scale bar, 20 mm. **g**, Growth seven days after inoculation of pearl oyster mushroom mycelium (white) on solid vermiculite substrate soaked with liquid YPD media containing simulated effluent in place of glucose (0.0691 M acetate: 1 M KOH) as indicated. Scale bar, 20 mm.

For the CO electrolyser, the operating current density of 150 mA cm^{-2} was selected to achieve greater than 80% conversion of electrochemically produced CO into C_{2+} products over the entire duration of electrolysis (Extended Data Fig. 1g,h). Initial experiments found that trace amounts of CO_2 negatively affected acetate selectivity in the CO electrolyser and led to a rapid increase in CO electrolyser voltage (Fig. 2b,c). When a 5 M NaOH scrubber was introduced between the two electrolysers, acetate selectivity was increased by over a factor of 3, because the scrubber prevented the unreacted CO_2 from the first reactor from reaching the CO electrolyser (Fig. 2d–f and Extended Data Fig. 1b). Overall, 57% of reacted CO_2 formed acetate at a production rate of 0.7 g d^{-1} cm^{-2}, representing the highest conversion of CO_2 feed to acetate reported to date (Fig. 2e and Supplementary Table 1).

The tandem CO_2 electrolysis system operated stably while producing effluent with high acetate-to-electrolyte ratios. The electrolyser voltage for the CO_2 electrolyser remained constant near 2.95 V (Fig. 2f) with less than a 60 mV increase in voltage over the six-hour experiment. The CO reactor operated at 2.22 V with a voltage increase of 160 mV over the course of the experiment (Fig. 2f), which is attributed to the pH shift in the electrolyte from 13.7 to 13.4 as acetate accumulated. Both catholyte (through the use of a cold-trap) and anolyte were collected and analysed for product quantification. As >99% of the produced acetate was collected in the anolyte, this was the primary effluent used for food production. The final effluent produced contained 0.75 M acetate and an acetate-to-electrolyte salt ratio of 0.75, representing the highest recorded acetate-to-electrolyte product stream to date (Supplementary Table 1).

Using CO_2 electrolysis to grow food heterotrophically. We used the photosynthetic alga *Chlamydomonas* (*C. reinhardtii*), which can grow heterotrophically on acetate in the dark, as a model to determine whether the improved effluent produced by the electrolysers could support the growth of food-producing organisms. *Chlamydomonas* is added to processed foods for protein fortification and has been shown to have a positive effect on human gastrointestinal health[24–28]. Algae can produce large amounts of starch, protein and oil. *Chlamydomonas* grown heterotrophically can produce over 1 g of starch, 1 g of protein and 0.7 g of lipid per litre per day[28,29]. To evaluate effluent as a carbon source, *Chlamydomonas* was grown heterotrophically in the dark with effluent diluted to match the acetate concentration of a typical liquid heterotrophic growth medium (17.5 mM acetate in Tris–acetate–phosphate (TAP) medium) and adjusted to pH 7.2. Effluent-derived acetate served as the sole carbon and energy source. Effluents from different electrolysis experiments used throughout this manuscript are noted by the acetate-to-electrolyte concentration ratio (acetate concentration: electrolyte concentration), with more details provided in Supplementary Table 2. All effluents evaluated with an acetate-to-electrolyte ratio of greater than 0.4 M acetate: 1 M electrolyte enabled the growth of *Chlamydomonas* in the dark

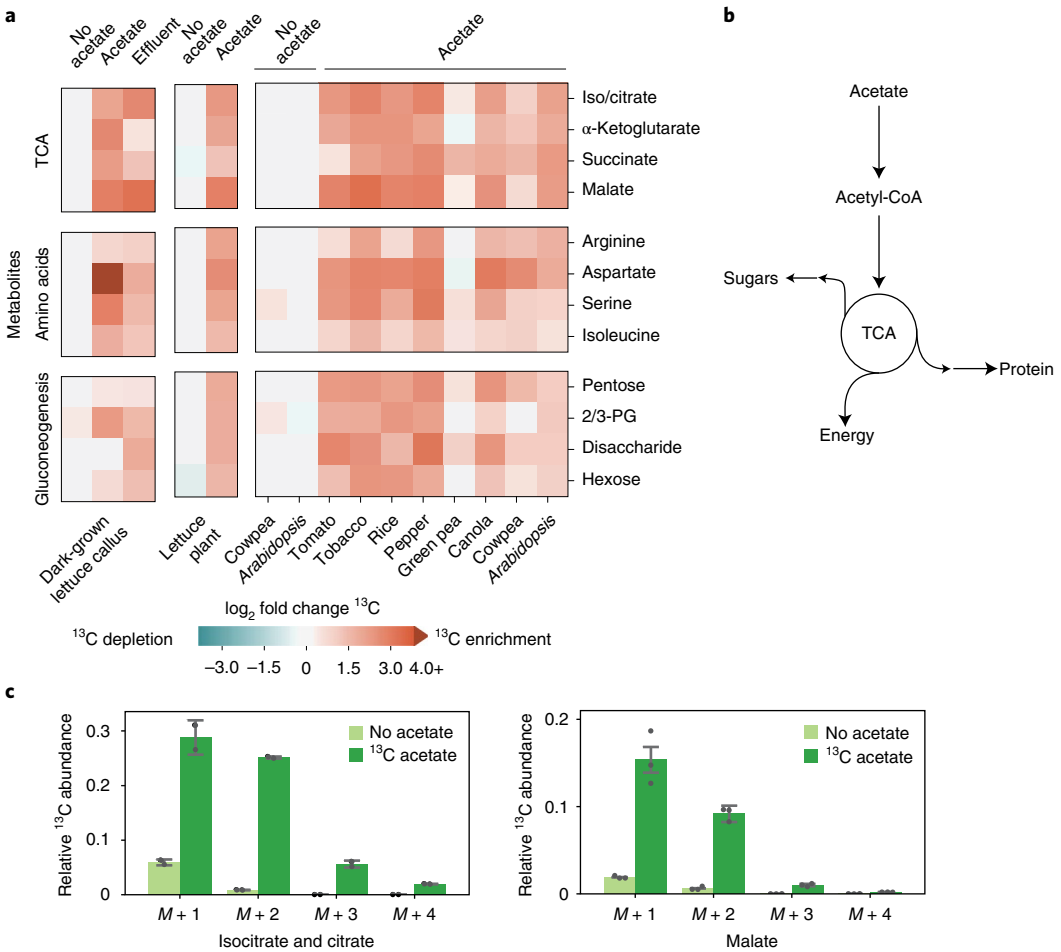

Fig. 4 | Lettuce and many other food-producing crop plants can utilize acetate for biomass and energy production. a, Heat maps showing the $\log_2$ fold enrichment of ^{13}C between treated and untreated whole lettuce plants and lettuce callus (undifferentiated lettuce). Whole lettuce plants were grown in the light and treated with no acetate or with ^{13}C-acetate ($n=3$; each replicate was a mixture of tissue from ten plants). Lettuce callus was grown in the dark and treated with electrolyser-produced effluent (0.691 M acetate: 1 M KOH) ($n=4$) and ^{13}C-acetate ($n=3$). A variety of crop species were treated with ^{13}C-acetate, and incorporation was measured. 2/3-PG, 2/3-phosphoglycerate. Representative no-acetate control replicates for whole lettuce plant, lettuce callus, cowpea and *Arabidopsis* are included for comparison. There was broad ^{13}C incorporation into crop metabolism, indicating that exogenously supplied acetate can be used for energy and biomass production in these plants. **b**, Schematic of exogenous acetate metabolism by a typical plant cell. **c**, ^{13}C incorporation into iso/citrate and malate at multiple carbon positions in whole lettuce plants. We calculated the ratio of iso/citrate and malate molecules that were detected with ^{13}C incorporation compared with ^{12}C. $M+X$ denotes the number of labelled carbons in the molecule. The error bars represent the standard deviation between the biological replicates ($n=3$).

(Supplementary Note, Fig. 3a–c, Extended Data Figs. 2 and 3a–e, and Supplementary Table 3).

Chlamydomonas grown on an effluent with an improved acetate-to-electrolyte salt ratio (0.75 M acetate: 1 M KOH) had a yield of 0.28 g algae per g acetate (Fig. 3b,c), which is comparable to yields reported from non-effluent medias[29]. *Chlamydomonas* utilized over 99% of acetate in the media (Extended Data Fig. 3f). No products of photosynthesis (such as carbohydrates) or ancient photosynthesis (such as petroleum-derived carbon sources) were required for growth. Hence, our cultivation of a photosynthetic organism using carbon fixed through electrolysis is fully decoupled from biological photosynthesis.

The nutritional yeast *Saccharomyces cerevisiae* is used as a food source in single-cell protein spreads and in the production of breads and fermented beverages[30,31]. Yeast is a heterotrophic organism most commonly grown with glucose derived from photosynthesis (that is, starch-derived) as a carbon and energy source. To cultivate yeast without inputs derived from photosynthesis, we replaced the primary carbon source, glucose, in the yeast–peptone–dextrose (YPD) media with effluent from electrolysis. All media were adjusted to pH 6.0. Electrolyser-produced effluent (0.75 M acetate: 1 M KOH) supported the growth of yeast, enabling a yield of 0.19 g yeast biomass per g acetate as well as a ninefold increase in OD600 and a twofold increase in dry weight compared with yeast grown without acetate or glucose (Fig. 3d,e). After successfully decoupling the production of yeast from photosynthesis-derived carbon and energy, we sought to achieve the same results in mushroom-producing fungus. Mushrooms are widely consumed as a food, and fungal mycelium has emerged as a high-protein meat analogue[32]. These fungi are typically cultivated on solid substrates composed of photosynthesis-derived carbohydrates, such as cellulose or rice flour. To cultivate fungal mycelium without these carbohydrates, we developed a solid-state fermentation approach that used effluent as the primary carbon and energy source. Due to the amounts needed, simulated effluents were used here, made up of the same components as electrolyser-produced effluents. Simulated effluent (0.691 M acetate: 1 M KOH) was added to YPD media without glucose to reach 0.5% (w/w) acetate; this substrate supported the

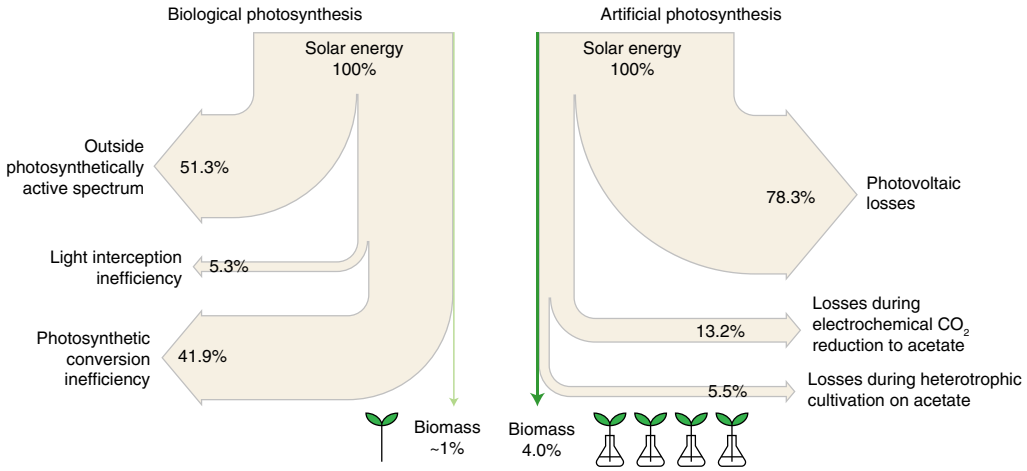

Fig. 5 | Artificial photosynthesis is more energy efficient than biological photosynthesis for plant- and algae-based food production. Sankey diagrams of solar energy to plant- and algae-based food production compare the efficiencies of artificial and biological photosynthesis. Losses during energy conversion from sunlight (100% solar energy) to food are represented by arrows; the width of each arrow is proportional to the energy lost, and the percentage of the total energy lost at each step is indicated. The green arrows indicate the solar energy that can be found in biomass grown from artificial and biological photosynthesis; the width of each arrow is proportional to the energy, and the percentage of the total solar energy found in the biomass is indicated. The values for biological photosynthesis are from Zhu et al.[57]. For artificial photosynthesis, the values for electrochemical CO_2 reduction to acetate and heterotrophic cultivation on acetate were determined in this work. The value for photovoltaic losses is based on a commercially available silicon solar cell[49,50].

growth of pearl oyster, blue oyster, elm oyster, coral tooth and enoki-take mycelium (Fig. 3f and Extended Data Fig. 3g–i). The majority of the substrate was fully colonized by all five species, indicating that effluent can serve as a carbon source for the cultivation of a variety of mushroom-producing fungus mycelia. Higher levels of effluent inhibited mycelium growth (Fig. 3g and Extended Data Fig. 3g), probably due to the higher levels of effluent by-products, specifically propionate, which is used as an antifungal food preservative[33]. The successful growth of mycelium indicates the ability to produce mycelium-based foods and potentially mushrooms independent of carbon and energy derived from photosynthesis.

Acetate can be metabolized by crop plants. To further evaluate whether carbon fixed through CO_2 electrolysis could be used to produce plant-based food, we examined the potential of acetate to serve as a carbon and energy source for crops. We tracked acetate incorporation into plant biomass using heavy-isotope ^{13}C-acetate labelled at both carbon atoms to evaluate whether exogenous acetate can be metabolized by crops. Previous acetate incorporation studies have primarily focused on metabolites involved in lipid biosynthesis in only a few plant species. In these studies, acetate was used in low concentrations as a tracer, not as a carbon source (Supplementary Table 4)[34–36]. To investigate acetate utilization as a carbon source, we grew undifferentiated lettuce tissue (callus) (to avoid the carbon and energy stored in seeds) in the dark in liquid media containing effluent (0.691 M acetate: 1 M KOH) and added in ^{13}C-acetate to enable tracking of carbon incorporation. Calli showed extensive ^{13}C-labelling in multiple pathways, confirming that lettuce tissue metabolizes acetate as a carbon and energy source (Fig. 4a). Labelling of citrate/isocitrate, succinate, α-ketoglutarate and malate indicated that exogenous acetate was converted to biologically active acetyl-CoA and entered the tricarboxylic acid cycle (TCA) cycle to produce energy (GTP, NADH and $FADH_2$) (Fig. 4a). Amino acids were also labelled with ^{13}C, indicating that carbon from acetate can be used to build proteins. Products and intermediates of gluconeogenesis were also labelled, indicating that carbon from acetate can be used for carbohydrate biosynthesis (Fig. 4a and Extended Data Fig. 4). Carbon incorporation of ^{13}C-acetate into amino acids and sugars through the TCA cycle, glycolysis and gluconeogenesis provides strong evidence that exogenous acetate can be readily incorporated into the bulk biomass of lettuce tissue grown in dark conditions and could be a carbon and energy source for other crops.

To test acetate uptake and utilization by whole plants, we grew lettuce plants in the light with ^{13}C-acetate added to the plant growth agar medium at 2 mM. In vegetative leaf tissue, we observed that amino acids, sugars and intermediates from the TCA cycle, glycolysis and gluconeogenesis were labelled with ^{13}C at multiple carbon positions (Fig. 4a–c). Finding labelled metabolites in leaf tissue indicates that carbon from acetate assimilated by the roots can be distributed throughout the plant. In addition to lettuce, we discovered that acetate can be incorporated into a broad variety of crops. Rice, green pea, jalapeño pepper, canola, tomato, cowpea, tobacco and *Arabidopsis* seedlings grown in the light on solid agar containing ^{13}C-acetate all showed similar ^{13}C-labelling of amino acids, carbohydrates and TCA cycle intermediates (Fig. 4a and Extended Data Fig. 5) as was observed in lettuce and lettuce callus. This metabolite labelling pattern suggests a conserved mechanism of acetate utilization that exists across diverse plant species.

Lettuce seeds germinated normally on all concentrations of acetate evaluated (up to 10 mM) (Extended Data Fig. 6a,b). However, plant growth was largely inhibited by acetate at concentrations that would have measurably increased plant biomass, although some growth parameters such as roots showed increased growth (Extended Data Figs. 6 and 7). Lettuce plants grown with electrolyser-produced effluent (0.691 M acetate: 1 M KOH or 0.648 M acetate: 1 M $KHCO_3$) added to reach a final media concentration of 1.0 mM acetate did not show additional growth inhibition in plant weight or leaf number from secondary electrolysis products (Extended Data Fig. 7b,d). Plant tolerance and consumption of acetate as a heterotrophic energy source will need to be increased to fully decouple plants from biological photosynthesis. Together, these analyses explore acetate as a heterotrophic carbon source for crops and illustrate that many crop species can process acetate into a usable biological form and incorporate it into major energy-production cycles through TCA and biomass in the form of sugars and amino acids.

Discussion

We demonstrated a hybrid inorganic–biological system that can produce food from carbon dioxide and electricity, independent of biological photosynthesis. CO_2 electrolysis for acetate production was significantly improved for the purpose of biological integration. Using a two-step process, we achieved electrochemical reduction of CO_2 to acetate with a 57% carbon selectivity towards acetate, the highest published value to date. The electrolysis system was further engineered to produce improved effluents with acetate-to-electrolyte salt ratios as high as 0.75, well above the ratio determined necessary to support biological growth. Electrochemically derived acetate was incorporated into a diverse variety of organisms grown for food, including algae, fungi and crop plants. This includes the cultivation of a photosynthetic organism, *Chlamydomonas*, utilizing carbon fixed through electrolysis, independent of biological photosynthesis. ^{13}C-labelling experiments showed that a broad range of crops can utilize exogenous acetate for energy and biomass production, suggesting that acetate has the capacity to support crop growth with further optimization.

By powering electrolysis with photovoltaics, the conversion of sunlight and CO_2 to food in our system (photovoltaics to electrolysis to acetate to yeast) is almost 18 times more solar-to-biomass energy-conversion-efficient than typical food production, which relies on biological photosynthesis (photosynthesis to glucose to yeast) (Extended Data Fig. 8). For algae production, our process (photovoltaics to electrolysis to acetate to algae) is almost four times more solar-to-biomass energy-conversion-efficient than biological photosynthesis of crop plants (photosynthesis to crop plants) and is equivalent to or higher than the instantaneous energy efficiency of outdoor algae production[37] (Fig. 5 and Extended Data Fig. 8). There is potential for continued improvement of the system through advances in photovoltaics, electrolysis and acetate utilization in food-producing organisms. Our approach to food production is ideally suited for applications where high energy efficiencies and low physical space usage are desired, such as on space flight missions or in controlled environments on Earth. Widespread adoption of this approach in conjunction with readily available solar energy could allow for the production of more food or animal feed for a given solar footprint, which will help meet the rising demand for food without the expansion of agricultural lands.

Methods

Electrolysis methods. *Cathode preparations.* For the CO_2 reduction electrodes, commercial silver (Ag) catalysts (nanopowder with <100 nm particle size, 99.5%) were purchased from Sigma Aldrich. Catalyst ink was prepared by suspending 100 mg of Ag nanopowder in 20 ml of 2:1 (v:v) isopropanol/deionized water. The suspension was sonicated for five minutes to allow complete dispersion of Ag particles. Afterwards, Sustanion XA-9 ionomer (5% (w/w) in ethanol, Dioxide Materials) was added until the ionomer reached 10% (w/w) in solution (metal basis). The resulting mixture was further sonicated for an additional 30 minutes to allow complete dispersion. To prepare the electrodes, a 25 cm^2 piece of Sigracet 39BB gas carbon paper (Fuel Cell Store), used as a gas diffusion layer, was heated on a hot plate to 100 °C. Catalyst ink was airbrushed onto the carbon paper until a loading of 1.4 mg cm^{-2} was reached. The electrode was dried at 70 °C overnight to ensure the complete evaporation of solvents.

For the CO reduction electrodes, commercial copper (Cu) catalyst (nanopowder with 25 nm particle size (TEM)) was purchased from Sigma Aldrich. Catalyst ink was prepared by suspending 100 mg of Cu nanopowder in 20 ml of 2:1 (v:v) isopropanol/deionized water. The suspension was sonicated for five minutes to allow complete dispersion of Cu particles. Afterwards, Sustanion XA-9 ionomer (5% (w/w) in ethanol, Dioxide Materials) was added until the ionomer reached 20% (w/w) in solution (metal basis). The resulting mixture was further sonicated for an additional 30 minutes to allow complete dispersion. To prepare the electrodes, a 5 cm^2 piece of Sigracet 39BB carbon paper (Fuel Cell Store) was heated on a hot plate to 100 °C. Catalyst ink was drop-casted onto the carbon paper until a loading of 2.0 mg cm^{-2} was reached. The electrode was dried at 70 °C overnight to ensure the complete evaporation of solvents.

Anode preparations. For experiments using 1 M $KHCO_3$, IrO_2 catalysts were prepared via a previously reported method[38]. In a typical preparation, titanium felt (Fuel Cell Store) was degreased using acetone and etched in boiling 0.5 M oxalic acid (98%, Sigma Aldrich). The titanium felt was then dip-coated in a solution of 10 ml of isopropanol, 10 vol% concentrated HCl (ACS reagent, Sigma Aldrich), containing 30 mg dissolved $IrCl_3{\cdot}xH_2O$ (99.8%, Alfa Aesar). This was followed by drying at 100 °C for ten minutes and calcination at 500 °C for ten minutes. This procedure was repeated until a loading of 3 mg cm^{-2} was achieved.

For experiments conducted in alkaline conditions, $NiFeO_x$ anodes prepared by a previously reported method[39] were used. In a typical preparation, Ni foam (>99.99%, MTI Corporation) was sonicated in a 5 M HCl solution for 30 minutes to remove the NiO_x layer on the surface. The foam was then rinsed using deionized water and ethanol and dried in air. Electrodeposition was carried out in a standard three-electrode electrochemical reactor containing the nickel foam as the working electrode, a platinum wire counter electrode and a Ag/AgCl (Pine Research) reference electrode. The electrolyte bath contained 3 mM $Ni(NO_3)_2{\cdot}6H_2O$ and 3 mM $Fe(NO_3)_3{\cdot}9H_2O$. A constant potential of −1.0 V versus Ag/AgCl was applied for 300 seconds. The electrode was then removed and rinsed with ethanol and deionized water, followed by drying overnight at 70 °C to fully remove solvents. A fresh cathode was used for each experiment, whereas the anodes were reused multiple times.

Flow electrolyser. Both the CO_2 and CO electrolysers were constructed as 5 cm^2 membrane electrode assemblies with serpentine flow patterns. The cathode end plates and the CO_2 electrolyser anode end plate were gold-plated stainless steel. The CO electrolyser anode end plate was not gold coated, as stainless steel is stable in alkaline conditions. The CO_2 gas flow rate into the electrolysers was controlled via a Brooks GF040 and held at 7 ml min^{-1} for the two-step experiments. The back pressure was controlled using a back-pressure controller (Cole-Palmer). The anolyte flow rates for both electrolysers were controlled via a peristaltic pump, with flow rates ranging between 0.5 and 1 ml min^{-1}. A cold trap chilled using ice was placed between the gas outlet stream of the CO electrolyser and the back-pressure controller to capture any vaporized liquid products that might exit through the gas stream.

For the CO_2 electrolyser, the Ag cathode and the IrO_2 anode were pressed into a Sustanion 37-50 Anion Exchange Membrane (Dioxide Materials) at 20 lb-in torque. Laser-cut Teflon (McMaster Carr) was used as a gasket to ensure that the electrolyser was gas-tight. 1 M $KHCO_3$ was used as the anolyte for all CO_2 reduction experiments. A constant current was applied using a power source (National Instruments). For the CO electrolyser, the Cu cathode and the IrO_2 or $NiFeO_x$ anode were pressed against an FAA-3-50 anion exchange membrane (Fumatech) at 20 lb-in torque. 1 M $KHCO_3$ or 2 M KOH was recirculated through the anode chamber. Liquid products were accumulated in the anolyte of the CO electrolyser until a target concentration was reached. The quantification of liquid products was conducted at the end of the experiment. For the CO electrolyser, the applied current was controlled using an Autolab PG128N potentiostat (Metrohm).

Gas products were quantified using a Multiple Gas Analyzer No. 5 gas chromatography system (SRI Instruments) equipped with a HaySep D and Molsieve 5 A column connected to a thermal conductivity detector. All gas products were quantified using the thermal conductivity detector data. Liquid products were quantified using a Bruker AVIII 600 MHz NMR spectrometer. Typically, 20 to 100 µl of collected electrolyte exiting the reactor was diluted to 500 µl, and then 100 µl D_2O containing 20 ppm (m/m) dimethyl sulfoxide (≥99.9%, Alfa Aesar) was added. One-dimensional ^1H spectrum was measured with water suppression using a pre-saturation method.

Effluents containing all liquid products were used for the growth of food-producing organisms. Electrolyser-produced effluents were used when possible, but in some cases simulated effluents of the same makeup were used.

Algae methods. *Chlamydomonas reinhardtii* (strain 21gr+, CC-1690 from the Chlamydomonas Resource Center) was cultivated on TAP media[40] where the source of acetate was a commercial supplier (Sigma 64-19-7), simulated effluent, electrolyser-produced effluent or none at all. When effluent (electrolyser produced or simulated) was the acetate source, it was added until the desired final acetate concentration was reached (17.5 mM). Ethanol (Koptec 64-17-5), propionic acid (Sigma 79-09-4) and *n*-propanol (Sigma 71-23-8) were added as indicated in Supplementary Table 3. All media were adjusted to pH 7.2 with 5 M HCl. Effluents and media concentrations are shown in Supplementary Tables 2 and 3.

Chlamydomonas was grown in 50 ml of media in 250 ml flasks in the dark. The flasks were stationary at 22 °C except for the experiment using 0.75 M acetate: 1 M KOH (data in Fig. 3b,c), where the flasks were at 30 °C with a shaking speed of 150 r.p.m.[29]. Aliquots were taken in a darkened biosafety cabinet and used for OD measurements at wavelength 750 nm (QuickDrop Spectrophotometer, Molecular Devices), chlorophyll extraction and quantification[41], and cell counts using a haemocytometer or the Bio-Rad TC20 Automated Cell Counter. For dry cell weights, the entire culture was centrifuged, washed two times with deionized water to remove residual salts, dried overnight at 100 °C and then weighed. Images were taken with a Nikon 7500 DSLR camera.

Yeast and mushroom methods. *Saccharomyces cerevisiae* was cultured in a base medium of yeast extract (10 g l^{-1}) and peptone (20 g l^{-1}) with glucose, effluent or no additional primary carbon source[42]. Standardized comparisons of acetate and glucose were made on the basis of energy content, and a variety of glucose

and effluent concentrations were tested, as shown in Supplementary Table 5. The highest concentration is based on 2% sodium acetate[42]. Media with a carbon source with the energetic equivalent of 53.36 kJ l^{-1} (0.061 M glucose or 0.019 M acetate) were determined to be the most efficient and thus were used in the yeast experiments shown in Fig. 3d,e. All media were adjusted to pH 6.0 with 5 M HCl. Cells were grown in 5 ml of media in culture tubes at 30 °C and 251 r.p.m. Growth was monitored by measuring OD at 600 nm and dry cell weight at 96 hours. For dry weights, the pellet was washed with deionized water to remove residual salts, dried overnight at 100 °C and then weighed. Effluents and media concentrations are shown in Supplementary Tables 2 and 3.

For the cultivation experiments with mushroom-producing fungi, the following five species were used: pearl oyster (*Pleurotus ostreatus*), elm oyster (*Hypsizygus ulmarius*), blue oyster (*Pleurotus ostreatus* var. columbinus), enokitake (*Flammulina velutipes*) and coral tooth (*Hericium coralloides*). The strains were purchased from liquidfungi.com and maintained on a liquid medium of glucose, yeast extract and peptone. Fungal mycelia were grown in a solid-state fermentation approach that roughly followed the PF-Tek methodology[43]; however, the carbon sources typically added, such as starch (rice flour), peat moss and coconut fibre, were omitted. A solid substrate of fine-grade vermiculite (30 g) was mixed with gypsum (0.5 g) and added to a 10 oz wide-mouth mason jar (Kamota). Liquid growth media (90 ml) were added to each jar, which soaked into the vermiculite. Media composition was the same as the maintenance media except that the carbon source was glucose (20 g l^{-1}), acetate (as indicated), effluent (as indicated), no carbon source or a combination of these. Media pH was adjusted to 6.0 with HCl. The jars were closed with lids with four drilled holes (12.7 mm in diameter) covered with a synthetic filter disk (0.3 µm pore size) to allow gas exchange. The jars were autoclaved for 45 minutes at 121 °C. Liquid mycelium cultures were centrifuged, washed with sterilized media, resuspended and then used to inoculate the sterilized jars.

Plant methods. *Plant material, media and growth conditions.* The following nine plants were used: lettuce (*Lactuca sativa* L. cv. 'Black Seeded Simpson'), rice (*Oryza sativa* ssp. *japonica* cv. 'Kitaake'), green pea (*Pisum sativum*), tomato (*Solanum lycopersicum* cv. 'Micro-Tom'), jalapeño pepper (*Capsicum annuum* cv. 'Jalapeño'), canola (*Brassica napus*), cowpea (*Vigna unguiculata* L. cv. CB46), thale cress (*A. thaliana* var. 'Columbia') and tobacco (*Nicotiana tabacum* cv. *Xanthi*).

Plants were cultivated on 50 ml of basal medium of 1/2 Murashige and Skoog salts[44] (Caisson Labs) and Gamborg's vitamins[45] (Phytotech Labs), unless otherwise noted. Solid media were made with 0.7% in vitro growth-grade agarose (Caisson Labs). The following were added as indicated: sucrose (2%), acetic acid, $^{13}C_2$-acetate (Sigma Aldrich) or electrolyser-produced effluent. All media were adjusted to pH 5.8 using 1 M KOH or HCl. The plants were grown in 16:8-hour light–dark cycles under fluorescent lighting (100 µmol m^{-2} s^{-1}) at 22 °C, unless otherwise noted.

Acetate feeding experiment. Lettuce was germinated in soil for 11 days. The plants were clipped at the base of the stem and were further trimmed so that all lettuce stems were the same length for the start of the experiment. Each plant was transferred to an 8 ml glass vial containing deionized water with acetate dissolved at various concentrations (nine plantlets per treatment: 0, 0.1, 0.3, 0.6, 1, 3, 6 and 10 mM acetate). After 29 days, the plantlets were imaged (using a Nikon 7500 DSLR with an AF-S VR Micro-Nikkor 105 mm f/2.8 G IF-ED lens) and removed from the solution for measurement of leaf number, stem length, root length and fresh weight. Stem length was measured from the first lateral root to the tip of the stem, and roots were measured on the basis of the longest root on the plantlet.

Experimental setup for plant germination and ^{13}C exposure. For the lettuce germination experiments, seeds were sterilized using a 15% bleach solution and a drop of Tween for every 50 ml of sterilizing solution. The seeds were incubated in the sterilizing solution for 15 minutes while shaking and then washed five times with sterile water, five minutes for each wash while shaking. Ten lettuce seeds were placed on agar basal media (25 ml) supplemented with acetate (0.1, 0.3, 0.6, 1, 2, 3, 6 or 10 mM), with 2 mM labelled $^{13}C_2$-acetate or with no additions to the base medium. They were allowed to germinate and grow for 28 days and were then imaged and removed to measure stem length, leaf number and fresh weight (not including the roots). Tissue samples for the ^{13}C-labelling experiments and the untreated controls were frozen in liquid nitrogen and stored at −80 °C until they were used for metabolomic analysis. For the other plant species, the same sterilization procedure was used for the seeds, and the plants were grown until there was at least a few hundred milligrams of tissue for metabolomic analysis (canola, 14 days; rice, 14 days; *Arabidopsis*, 18 days; Micro-Tom tomato, 22 days; green pea, 22 days; *Nicotiana benthamiana*, 32 days; cowpea, 32 days).

Lettuce callus in liquid culture. Undifferentiated lettuce callus was generated by plating pieces of lettuce leaf tissue on callus-inducing media (1/2 Murashige and Skoog salts, 0.05 mg l^{-1} α-naphthaleneacetic acid, 0.4 mg l^{-1} 6-benzyl aminopurine and Gamborg's vitamins[45]) (Phytotech Labs). The calli were cut to the desired size and weighed to ensure that an equal amount of tissue was added to each flask. Each flask of calli was incubated in liquid 1/2 Murashige and Skoog media supplemented with acetate, $^{13}C_2$-acetate or sucrose (2%) as indicated and to the specified concentrations. All cultures were grown at 22 °C in the dark at 100 r.p.m. Tissue samples for the ^{13}C-labelling experiment and control samples were frozen in liquid nitrogen and stored at −80 °C until they were used for metabolomic analysis.

Metabolomic analysis. *Sample preparation.* Plant tissue was freeze-dried, and then approximately 10 mg was weighed into a 2 ml tube and homogenized using a bead mill, using three 2.8 mm beads per tube. To each sample, 750 µl of 1:2 water:methanol was added, and the samples were then vortexed for 60 min at 4 °C. Then, 500 µl of chloroform was added, and the samples were vortexed at 4 °C for an additional 15 min. After centrifugation for 10 min (16,000 *g* at 4 °C), the top, polar layer was transferred to a glass vial and analysed by liquid chromatography–mass spectrometry (LC–MS).

LC–MS. LC–MS metabolomics analysis was performed at the University of California, Riverside Metabolomics Core Facility. The analysis was performed on a Synapt G2-Si quadrupole time-of-flight mass spectrometer (Waters). Metabolite separations were carried out on an I-class UPLC system (Waters) using a ZIC-pHILIC column (2.1 mm × 150 mm, 5 µM) (EMD Millipore). The two mobile phases used were (A) water with 15 mM ammonium bicarbonate adjusted to pH 9.6 with ammonium hydroxide and (B) acetonitrile. The column was held at 20 °C, and the flow rate was 150 µl min^{-1}. The sample injection volume was 2 µl. The following gradient was performed: 0 min, 10% A, 90% B; 1.5 min, 10% A, 90% B; 16 min, 80% A, 20% B; 29 min, 80% A, 20% B; 31 min, 10% A, 90% B; 32 min, 10% A, 90% B.

The mass spectrometer was operated in negative ion mode (50 to 1200 *m*/*z*) with a 100 ms scan time. Tandem MS was acquired in a data-dependent fashion. The source temperature was 150 °C, and the desolvation temperature was 600 °C. Nitrogen was used as a desolvation gas (1,100 l h^{-1}) and cone gas (150 l h^{-1}). The collision gas used was argon. The capillary voltage was 2 kV. Leucine enkephalin was infused and used for mass correction.

Data processing and analysis. Data processing was performed with the open-source Skyline software[46]. Metabolites were identified by MS (less than 5 ppm) and tandem MS using the Metlin database[47]. Data for isocitrate and citrate and for 2-phosphoglycerate and 3-phosphoglycerate are included as cumulative values (iso/citrate and 2/3-phosphoglycerate) because they are not distinguishable through the LC–MS methodology used. The $\log_2$ ^{13}C enrichment was calculated for the heat maps using the equation:

$$\log_2\left(\frac{\text{treatment}\left(\frac{M+X}{M}\right)}{\text{control}\left(\frac{M+X}{M}\right)}\right)$$

where M is the area under the curve measured by LC–MS of molecules made up of ^{12}C atoms only, and $M+X$ is the area under the curve measured by LC–MS of molecules with ^{13}C-isotope atoms incorporated into the molecule, X being the number of ^{13}C-isotope atoms incorporated. When multiple biological replicates were available, they were averaged before dividing treatment by control. The untreated control replicates shown are a single representative replicate normalized to the average of all replicates, which helps visualize any variation between controls.

Energy efficiency calculations. *Efficiency calculations for electrocatalysis.* The following equations were used to determine the efficiency of the electrolysis process. Faradaic efficiency (FE) from gas chromatography was calculated as

$$\text{FE}\,(\%) = \frac{n \times F \times x \times V}{j_{\text{Tot}}} \times 100$$

where n is the number of electrons transferred, F is Faraday's constant, x is the mole fraction of the product, V is the total molar flow rate of the gas and j_{Tot} is the total current. Liquid Faradaic efficiency was calculated using quantitative ^{1}H-NMR.

Carbon selectivity was calculated as

$$\text{Carbon selectivity}\,(\%) = \frac{n_i \times F \times j_i \times C_i}{\sum_i n_i \times F \times j_i \times C_i} \times 100$$

where n_i is the number of electrons transferred to product i, j_i is the partial current towards product i and C_i is the number of carbons in product i. This value represents the percentage of CO_2 reacted towards C_{2+} products found in a given product or the molar selectivity of a given product scaled to the number of carbons contained in it.

To determine the overall efficiency of the electrolysis process, we calculated the theoretical energy required to produce the C_{2+} products and divided that by the actual amount of energy it took to produce those C_{2+} products. The C_{2+} product distribution is shown in Supplementary Table 6, where we assume 1 g of the C_{2+} products.

Theoretical potentials were calculated using the following equation:

$$E^0 = \frac{\Delta G^0}{F \times n}$$

where E^0 is the theoretical potential, n is the number of electrons and ΔG^0 is the Gibbs free energy of reaction.

Theoretical energy was calculated as follows:

$$\text{Theoretical energy per 1 g of } C_{2+} \text{ products} = \sum_i E_i^0 \times F \times n_i \times \frac{m_i}{MW_i}$$

$$= 21.86 \text{ kJ}$$

where E_i^0 is the theoretical cell potential for species i, m_i is the mass produced of product i and MW_i is the molecular weight of product i. The values for E^0 and m can be found in Supplementary Table 6.

The actual energy input to produce 1 g of C_{2+} products is calculated using the following equation:

$$\text{Actual energy input per 1 g of } C_{2+} \text{ products}$$
$$= \text{Actual energy input for CO electrolyser}$$
$$+ \text{Actual energy input for } CO_2 \text{ electrolyser}$$
$$= 31.22 \text{ kJ} + 30.14 \text{ kJ} = 61.36 \text{ kJ}$$

$$\text{Actual energy input for CO electrolyser} = \frac{m_{AcO} \times n_{AcO} \times F \times E_{CO}}{MW_{AcO} \times FE_{AcO}}$$

$$= \frac{0.716 \text{ g} \times 4 \frac{\text{mol}}{\text{mol}} \times 96{,}485 \frac{\text{C}}{\text{mol}} \times 2.3 \text{ V}}{60.052 \frac{\text{g}}{\text{mol}} \times 0.339}$$

$$= 31.22 \text{ kJ}$$

where m_{AcO} is the mass of acetate produced to produce a total of 1 g of C_{2+} products at the Faradaic efficiencies calculated and listed in Supplementary Table 6, n_{AcO} is the number of moles of electrons passed per mole of acetate produced, E_{CO} is the measured cell potential for the CO electrolyser, MW_{AcO} is the molecular weight of acetate and FE_{AcO} is the measured Faradaic efficiency of acetate. For the CO_2 electrolyser:

$$\text{Actual energy input for } CO_2 \text{ electrolyser} = \frac{N_{CO} \times n_{CO} \times F \times E_{CO_2}}{FE_{CO}}$$

$$= \frac{0.045 \text{ mol} \times 2 \frac{\text{mol}}{\text{mol}} \times 96{,}485 \frac{\text{C}}{\text{mol}} \times 2.95 \text{ V}}{0.85}$$

$$= 30.14 \text{ kJ}$$

where N_{CO} is the moles of carbon monoxide necessary to produce a total of 1 g of C_{2+} products at the 92% (measured) conversion in the CO electrolyser, n_{CO} is the number of electrons passed per mol of carbon monoxide produced, E_{CO_2} is the measured cell potential for the CO_2 electrolyser and FE_{CO} is the measured Faradaic efficiency of carbon monoxide.

Using the values listed in Supplementary Table 6, the energetic efficiency was calculated by taking the ratio of the theoretical energy and the actual energy input per 1 g of product:

$$\text{Energy efficiency of } C_{2+} \text{ product production}$$
$$= \frac{\text{Theoretical energy per g of } C_{2+} \text{ products}}{\text{Actual energy input per g of } C_{2+} \text{ products}}$$
$$= \frac{21.86 \text{ kJ}}{61.36 \text{ kJ}} \times 100\%$$
$$= 35.62\%$$

Our tandem electrolysis process has an energy efficiency of 35.62% for the production of all C_{2+} products, which accounts for losses due to selectivity, conversion and overpotential. If you consider ethylene as a complete loss and consider only products in the effluent, the energy efficiency of C_{2+} product production is 24.26%. We next calculated the energy efficiency of the production of just acetate, as this is what is used as the energy and carbon source for algal and yeast growth. To calculate acetate efficiency, we did not include losses due to selectivity because in a commercial setting, the other C_{2+} products (for example, ethylene) would be considered co-products of the process. The efficiency numbers including ethylene as a co-product were used to calculate the energy efficiency of the whole system. More details are shown below:

$$\text{Theoretical energy per 1 g acetate} = E_{AcO}^0 \times F \times n_{AcO} \times \frac{m_{AcO}}{MW_{AcO}} + E_{CO}^0$$
$$\times F \times n_{CO} \times \left(\frac{\text{mol}_{CO}}{\text{mol}_{AcO}} \times \frac{m_{AcO}}{MW_{AcO}}\right)$$
$$= 0.73 \text{ V} \times 96{,}485 \frac{\text{C}}{\text{mol}} \times 4 \frac{\text{mol}}{\text{mol}} \times \frac{1 \text{ g}}{60.052 \frac{\text{g}}{\text{mol}}} + 1.333 \text{ V} \times 96{,}485 \frac{\text{C}}{\text{mol}}$$
$$\times 2 \frac{\text{mol}}{\text{mol}} \times \left(2 \times \frac{1 \text{ g}}{60.052 \frac{\text{g}}{\text{mol}}}\right)$$
$$= 4.70 \text{ kJ} + 8.57 \text{ kJ} = 13.27 \text{ kJ}$$

$$\text{Actual energy input for CO electrolyser} = \frac{m_{AcO} \times n_{AcO} \times F \times E_{CO}}{MW_{AcO}}$$
$$= \frac{1 \text{ g} \times 4 \frac{\text{mol}}{\text{mol}} \times 96{,}485 \frac{\text{C}}{\text{mol}} \times 2.3 \text{ V}}{60.052 \frac{\text{g}}{\text{mol}}} = 14.78 \text{ kJ}$$

$$\text{Actual energy input for } CO_2 \text{ electrolyser} = N_{CO} \times n_{CO} \times F \times E_{CO_2}$$
$$= \left(2 \times \frac{1 \text{ g AcO}}{60.052 \frac{\text{g}}{\text{mol}}}\right) \times 2 \frac{\text{mol}}{\text{mol}} \times 96{,}485 \frac{\text{C}}{\text{mol}} \times 2.95 \text{ V}$$
$$= 18.96 \text{ kJ}$$

$$\text{Actual energy input per 1 g of acetate } (E_{AcO})$$
$$= \text{Actual energy input for CO electrolyser}$$
$$+ \text{Actual energy input for } CO_2 \text{ electrolyser}$$
$$= 14.78 \text{ kJ} + 18.96 \text{ kJ} = 33.71 \text{ kJ}$$

$$\text{Energy efficiency of acetate production} = \frac{\text{Theoretical energy per 1 g of acetate}}{\text{Actual energy input per 1 g of acetate}}$$
$$= \frac{13.27 \text{ kJ}}{33.71 \text{ kJ}} \times 100\% = 39.37\%$$

Efficiency calculations for food production. The efficiency values reported here are based on the statistical averages of at least three biological replicates. These calculations were conducted similarly to the approaches in Blankenship et al.[1] and Nangle et al.[48].

Energy efficiency of the heterotrophic cultivation of Chlamydomonas without inputs from biological photosynthesis. The energy efficiency of biological photosynthesis is defined as the energy content of the biomass that can be harvested annually divided by the annual solar irradiance over the same area[1]. To be able to compare our process to biological photosynthesis, we calculated the conversion efficiency of sunlight to biomass using photovoltaics to power our process of the electrolytic production of acetate followed by the heterotrophic cultivation of *Chlamydomonas* in the dark. We define the energy efficiency as the increase in biomass energy content divided by the required solar energy input. The increase in biomass energy content is calculated as

$$\text{Increase in algal biomass energy content} = \Delta X_{biomass} \times \Delta H^{\circ}_{biomass}$$
$$= (0.3733 \text{ g l}^{-1} - 0.0776 \text{ g l}^{-1}) \times (21.5 \text{ kJ g}^{-1})$$
$$= 6.36 \text{ kJ l}^{-1}$$

where $\Delta X_{biomass}$ is the gain of algal biomass and $\Delta H^{\circ}_{biomass}$ is the enthalpy of combustion of algal biomass, which was determined experimentally using an oxygen bomb calorimeter. The required solar energy input is calculated as

$$\text{Solar energy required} = \frac{\text{Acetate used} \times \text{Energy for acetate electrocatalysis}}{\text{Annual photovoltaic efficiency}}$$
$$= \frac{(C_{AcO} \times MW_{AcO} \times w_{consumed}) \times E_{AcO}}{\eta_{AM\ 1.5} \times \eta_{annual}}$$
$$= \frac{\left(0.01748 \text{ M acetate} \times 60.052 \frac{\text{g acetate}}{\text{mol}} \times 99.5\%\right) \times 33.71 \frac{\text{kJ}}{\text{g acetate}}}{22.8\% \times 95\%}$$
$$= 162.55 \text{ kJ l}^{-1}$$

where C_{AcO} is the acetate concentration in the algal media, MW_{AcO} is the molecular weight of acetate, $w_{consumed}$ is the fraction of acetate consumed by the algae, E_{AcO} is the energy required to generate acetate in the electrolyser (calculated above), $\eta_{AM1.5}$ is the maximum power conversion efficiency (peak solar intensity, AM1.5 spectral distribution) of a commercially available silicon solar cell (from Canadian Solar[49,50]) and η_{annual} is the photovoltaic annual efficiency, which is about 95% of the maximum power conversion efficiency value due to the changing solar zenith angle throughout the day and year[1]. The energy efficiency is then calculated as

$$\text{Energy efficiency of algae production} = \frac{\text{Increase in algal biomass energy content}}{\text{Solar energy required}}$$
$$= \frac{6.36 \text{ kJ l}^{-1}}{162.55 \text{ kJ l}^{-1}} = 3.91\%$$

Comparison of this number with the ~1% annual efficiency for most crop plants[1] shows that our approach can be almost four times more energy efficient than biological photosynthesis for the cultivation of photosynthetic organisms. Improvements in photovoltaic maximum power conversion efficiency would increase the efficiency of our approach. For example, multi-junction solar cells have been shown to reach efficiencies as high as 47.1%[49], which coupled to our system would bring the overall energy efficiency of sunlight to food to ~9%.

For Fig. 5 and Extended Data Fig. 8, we calculated the energy efficiencies at each step within the system as follows:

$$\text{Solar to electricity efficiency} = \eta_{\text{AM 1.5}} \times \eta_{\text{annual}}$$
$$= 22.8\% \times 95\% = 21.7\%$$

$$\text{Acetate to algal biomass efficiency} = Y_{\text{algae/acetate}} \times \frac{\Delta H^{\circ}_{\text{biomass}}}{\Delta H^{\circ}_{\text{AcO}}}$$
$$= 0.2831 \frac{\text{g yeast}}{\text{g acetate}} \times \frac{21.5 \text{ kJ g}^{-1}}{14.58 \text{ kJ g}^{-1}} = 41.75\%$$

where $Y_{\text{algae/acetate}}$ is the yield of algae grown with acetate effluent media, and $\Delta H^{\circ}_{\text{AcO}}$ is the enthalpy of combustion of acetate.

Energy efficiency of the cultivation of yeast. Nutritional yeast is heterotrophic and is typically cultivated with glucose derived from biological photosynthesis as the primary carbon and energy source. In our process, electrolysis-derived acetate is substituted for glucose. To compare these two ways to produce yeast, we calculated the amount of yeast that could be produced per area of land in Illinois, a large corn-producing state in the United States. To calculate the amount of yeast that could be produced by our process independent of biological photosynthesis, we used the annual average solar irradiance in Illinois to calculate the electricity that could be generated by photovoltaics to synthesize acetate in the CO_2 electrolyser and subsequently used to cultivate yeast, as follows:

$$\text{Yeast produced by artificial photosynthesis} = \text{Available energy from photovoltaics}$$
$$\times \text{Acetate electrocatalysis} \times \text{Yeast yield}$$
$$= (E_e \times \eta_{\text{AM1.5}} \times \eta_{\text{annual}}) \times (E_{\text{AcO}})^{-1} \times \left(Y_{\text{yeast/acetate}}\right)$$
$$= \left(5{,}543{,}620 \text{ kJ m}^{-2} \text{ yr}^{-1} \times 22.8\% \times 95\%\right) \times \left(33.71 \frac{\text{kJ}}{\text{g acetate}}\right)^{-1}$$
$$\times \left(0.1889 \frac{\text{g yeast}}{\text{g acetate}}\right)$$
$$= 6.73 \text{ kg yeast per m}^2 \text{ per yr}$$

where E_e is the average annual solar irradiance from the North America Land Data Assimilation System Daily Sunlight (kJ m^{-2}) dataset for Illinois from 2000 to 2011[51]; $\eta_{\text{AM1.5}}$ is the maximum power conversion efficiency (peak solar intensity, AM1.5 spectral distribution) of a commercially available silicon solar cell[49]; η_{annual} is the photovoltaic annual efficiency, which is about 95% of the maximum power conversion efficiency value due to the changing solar zenith angle throughout the day and year[2]; E_{AcO} is the energy required to generate acetate in the electrolyser (calculated above); and $Y_{\text{yeast/acetate}}$ is the yield of yeast grown with acetate effluent media.

To calculate the amount of yeast that could be produced per area of land with biological photosynthesis, we used the annual corn harvest data from Illinois to determine the glucose that could be generated by photosynthesis and subsequently used as the primary carbon and energy source to cultivate yeast, as follows:

$$\text{Yeast produced by biological photosynthesis}$$
$$= \text{Glucose produced by corn} \times \text{Yeast yield}$$
$$= \left(Y_{\text{corn per m}^2} \times Y_{\text{glucose/corn}}\right) \times \left(Y_{\text{yeast/glucose}}\right)$$
$$= \left(0.0423 \frac{\text{bu corn}}{\text{m}^2 \text{ yr}} \times 17.45 \frac{\text{kg glucose}}{\text{bu corn}}\right) \times \left(0.51 \frac{\text{g yeast}}{\text{g glucose}}\right)$$
$$= 0.376 \text{ kg yeast per m}^2 \text{ per yr}$$

where $Y_{\text{corn per m}^2}$ is the average corn kernel production in Illinois per square meter[52], $Y_{\text{glucose/corn}}$ is the glucose produced from a bushel of corn kernels[53] and $Y_{\text{yeast/glucose}}$ is the yield of yeast grown with glucose as the carbon source[54]. Using our artificial photosynthesis approach, almost 18 times more yeast could be produced per area of land.

For Extended Data Fig. 8, we calculated the energy efficiencies at each step within the systems as follows:

$$\text{Acetate to yeast biomass efficiency} = Y_{\text{yeast/acetate}} \times \frac{\Delta H^{\circ}_{\text{biomass}}}{\Delta H^{\circ}_{\text{AcO}}}$$
$$= 0.1889 \frac{\text{g yeast}}{\text{g acetate}} \times \frac{21.39 \text{ kJ g}^{-1}}{14.58 \text{ kJ g}^{-1}} = 27.7\%$$

$$\text{Sun to corn kernel efficiency} = \frac{Y_{\text{corn per m}^2} \times \Delta H^{\circ}_{\text{corn}}}{E_e}$$
$$= \frac{1.073 \text{ kg m}^{-2} \text{ yr}^{-1} \times 16{,}200 \text{ kJ kg}^{-1}}{5{,}543{,}620 \text{ kJ m}^{-2} \text{ yr}^{-1}} = 0.31\%$$

$$\text{Corn kernel to glucose efficiency} = w_{\text{glucose/corn}} \times \frac{\Delta H^{\circ}_{\text{glucose}}}{\Delta H^{\circ}_{\text{corn}}}$$
$$= 0.688 \times \frac{15.54 \text{ kJ g}^{-1}}{16.2 \text{ kJ g}^{-1}} = 66.0\%$$

$$\text{Glucose to yeast efficiency} = Y_{\text{yeast/glucose}} \times \frac{\Delta H^{\circ}_{\text{biomass}}}{\Delta H^{\circ}_{\text{glucose}}}$$
$$= 0.51 \frac{\text{g yeast}}{\text{g glucose}} \times \frac{21.39 \text{ kJ g}^{-1}}{15.57 \text{ kJ g}^{-1}} = 70.1\%$$

where $\Delta H^{\circ}_{\text{biomass}}$ is the enthalpy of combustion of yeast biomass[55], $\Delta H^{\circ}_{\text{kernel}}$ is the enthalpy of combustion of corn kernels[56], $w_{\text{glucose/corn}}$ is the mass fraction of glucose found in a corn kernel[53] and $\Delta H^{\circ}_{\text{glucose}}$ is the enthalpy of combustion of glucose.

There are many ways in which the energy of biological photosynthesis can be improved on, such as increasing CO_2 concentrations and metabolic engineering. We have included numbers for the theoretical maxima of both systems in Extended Data Fig. 8b (refs. [48–59]).

Reporting summary. Further information on research design is available in the Nature Research Reporting Summary linked to this article.

Data availability

The metabolomics data (Fig. 4a and Extended Data Figs. 4 and 5b) and all source data can be found at https://doi.org/10.6086/D1VT2V in the Dryad Digital Repository.

Received: 15 January 2022; Accepted: 9 May 2022;
Published online: 23 June 2022

References

1. Blankenship, R. E. et al. Comparing photosynthetic and photovoltaic efficiencies and recognizing the potential for improvement. *Science* **332**, 805–809 (2011).
2. Ort, D. R. et al. Redesigning photosynthesis to sustainably meet global food and bioenergy demand. *Proc. Natl Acad. Sci. USA* **112**, 8529–8536 (2015).
3. Kromdijk, J. et al. Improving photosynthesis and crop productivity by accelerating recovery from photoprotection. *Science* **354**, 857–861 (2016).
4. South, P. F., Cavanagh, A. P., Liu, H. W. & Ort, D. R. Synthetic glycolate metabolism pathways stimulate crop growth and productivity in the field. *Science* **363**, eaat9077 (2019).
5. Liu, C., Colón, B. C., Ziesack, M., Silver, P. A. & Nocera, D. G. Water splitting–biosynthetic system with CO_2 reduction efficiencies exceeding photosynthesis. *Science* **352**, 1210–1213 (2016).
6. Torella, J. P. et al. Efficient solar-to-fuels production from a hybrid microbial–water-splitting catalyst system. *Proc. Natl Acad. Sci. USA* **112**, 2337–2342 (2015).
7. Haas, T., Krause, R., Weber, R., Demler, M. & Schmid, G. Technical photosynthesis involving CO_2 electrolysis and fermentation. *Nat. Catal.* **1**, 32–39 (2018).
8. Yishai, O., Lindner, S. N., Gonzalez de la Cruz, J., Tenenboim, H. & Bar-Even, A. The formate bio-economy. *Curr. Opin. Chem. Biol.* **35**, 1–9 (2016).
9. Cai, T. et al. Cell-free chemoenzymatic starch synthesis from carbon dioxide. *Science* **373**, 1523–1527 (2021).
10. Woolston, B. M., King, J. R., Reiter, M., Van Hove, B. & Stephanopoulos, G. Improving formaldehyde consumption drives methanol assimilation in engineered *E. coli*. *Nat. Commun.* **9**, 2387 (2018).
11. Li, R., Moore, M., Bonham-Smith, P. C. & King, J. Overexpression of formate dehydrogenase in *Arabidopsis thaliana* resulted in plants tolerant to high concentrations of formate. *J. Plant Physiol.* **159**, 1069–1076 (2002).
12. Luc, W. et al. Two-dimensional copper nanosheets for electrochemical reduction of carbon monoxide to acetate. *Nat. Catal.* **2**, 423–430 (2019).
13. Gabardo, C. M. et al. Continuous carbon dioxide electroreduction to concentrated multi-carbon products using a membrane electrode assembly. *Joule* **3**, 2777–2791 (2019).
14. Lv, J.-J. et al. A highly porous copper electrocatalyst for carbon dioxide reduction. *Adv. Mater.* **30**, e1803111 (2018).
15. Li, C. W. & Kanan, M. W. CO_2 reduction at low overpotential on Cu electrodes resulting from the reduction of thick Cu_2O films. *J. Am. Chem. Soc.* **134**, 7231–7234 (2012).
16. de Arquer, F. P. G. et al. CO_2 electrolysis to multicarbon products at activities greater than 1 A cm^{-2}. *Science* **367**, 661–666 (2020).
17. Jouny, M., Luc, W. & Jiao, F. High-rate electroreduction of carbon monoxide to multi-carbon products. *Nat. Catal.* **1**, 748–755 (2018).
18. Ripatti, D. S., Veltman, T. R. & Kanan, M. W. Carbon monoxide gas diffusion electrolysis that produces concentrated C_2 products with high single-pass conversion. *Joule* **3**, 240–256 (2019).

19. Weekes, D. M., Salvatore, D. A., Reyes, A., Huang, A. & Berlinguette, C. P. Electrolytic CO_2 reduction in a flow cell. *Acc. Chem. Res.* **51**, 910–918 (2018).
20. Endrődi, B. et al. Multilayer electrolyzer stack converts carbon dioxide to gas products at high pressure with high efficiency. *ACS Energy Lett.* **4**, 1770–1777 (2019).
21. Ozden, A. et al. Cascade CO_2 electroreduction enables efficient carbonate-free production of ethylene. *Joule* **5**, 706–719 (2021).
22. Liu, Z., Yang, H., Kutz, R. & Masel, R. I. CO_2 electrolysis to CO and O_2 at high selectivity, stability and efficiency using sustainion membranes. *J. Electrochem. Soc.* **165**, J3371 (2018).
23. Romero Cuellar, N. S. et al. Two-step electrochemical reduction of CO_2 towards multi-carbon products at high current densities. J. CO_2 Util. **36**, 263–275 (2020).
24. Murbach, T. S. et al. A toxicological evaluation of *Chlamydomonas reinhardtii*, a green algae. *Int. J. Toxicol.* **37**, 53–62 (2018).
25. Kiataramgul, A. et al. An oral delivery system for controlling white spot syndrome virus infection in shrimp using transgenic microalgae. *Aquaculture* **521**, 735022 (2020).
26. Khemiri, S. et al. Microalgae biomass as an additional ingredient of gluten-free bread: dough rheology, texture quality and nutritional properties. *Algal Res.* **50**, 101998 (2020).
27. Fields, F. J. et al. Effects of the microalgae *Chlamydomonas* on gastrointestinal health. *J. Funct. Foods* **65**, 103738 (2020).
28. Torres-Tiji, Y., Fields, F. J. & Mayfield, S. P. Microalgae as a future food source. *Biotechnol. Adv.* **41**, 107536 (2020).
29. Zhang, Z. et al. Efficient heterotrophic cultivation of *Chlamydomonas reinhardtii*. *J. Appl. Phycol.* **31**, 1545–1554 (2019).
30. Ugalde, U. O. & Castrillo, J. I. in *Applied Mycology and Biotechnology* (eds Khachatourians, G. G. & Arora, D. K.) Vol. 2, 123–149 (Elsevier, 2002).
31. Pérez-Torrado, R. et al. Yeast biomass, an optimised product with myriad applications in the food industry. *Trends Food Sci. Technol.* **46**, 167–175 (2015).
32. Stephan, A., Ahlborn, J., Zajul, M. & Zorn, H. Edible mushroom mycelia of *Pleurotus sapidus* as novel protein sources in a vegan boiled sausage analog system: functionality and sensory tests in comparison to commercial proteins and meat sausages. *Eur. Food Res. Technol.* **244**, 913–924 (2018).
33. Brock, M. & Buckel, W. On the mechanism of action of the antifungal agent propionate. *Eur. J. Biochem.* **271**, 3227–3241 (2004).
34. Wang, P. et al. A ^{13}C isotope labeling method for the measurement of lignin metabolic flux in *Arabidopsis* stems. *Plant Methods* **14**, 51 (2018).
35. Dethloff, F., Orf, I. & Kopka, J. Rapid in situ ^{13}C tracing of sucrose utilization in *Arabidopsis* sink and source leaves. *Plant Methods* **13**, 87 (2017).
36. Allen, D. K., Bates, P. D. & Tjellström, H. Tracking the metabolic pulse of plant lipid production with isotopic labeling and flux analyses: past, present and future. *Prog. Lipid Res.* **58**, 97–120 (2015).
37. Melis, A. Solar energy conversion efficiencies in photosynthesis: minimizing the chlorophyll antennae to maximize efficiency. *Plant Sci.* **177**, 272–280 (2009).
38. Luc, W., Rosen, J. & Jiao, F. An Ir-based anode for a practical CO_2 electrolyzer. *Catal. Today* **288**, 79–84 (2017).
39. Lu, X. & Zhao, C. Electrodeposition of hierarchically structured three-dimensional nickel–iron electrodes for efficient oxygen evolution at high current densities. *Nat. Commun.* **6**, 6616 (2015).
40. Gorman, D. S. & Levine, R. P. Cytochrome *f* and plastocyanin: their sequence in the photosynthetic electron transport chain of *Chlamydomonas reinhardi*. *Proc. Natl Acad. Sci. USA* **54**, 1665–1669 (1965).
41. Harris, E. H., Stern, D. B. & Witman, G. B. *The Chlamydomonas Sourcebook* Vol. 2 (Academic Press San Diego, 1989).
42. Minard, K. I. & McAlister-Henn, L. Redox responses in yeast to acetate as the carbon source. *Arch. Biochem. Biophys.* **483**, 136–143 (2009).
43. Yachaj. Mushroom cultivation: from falconer to fanaticus and beyond. *Entheogen Rev.* **10**, 127–139 (2001).
44. Murashige, T. & Skoog, F. A revised medium for rapid growth and bio assays with tobacco tissue cultures. *Physiol. Plant.* **15**, 473–497 (1962).
45. Gamborg, O. L., Murashige, T., Thorpe, T. A. & Vasil, I. K. Plant tissue culture media. *In Vitro* **12**, 473–478 (1976).
46. MacLean, B. et al. Skyline: an open source document editor for creating and analyzing targeted proteomics experiments. *Bioinformatics* **26**, 966–968 (2010).
47. Guijas, C. et al. METLIN: a technology platform for identifying knowns and unknowns. *Anal. Chem.* **90**, 3156–3164 (2018).
48. Nangle, S. N. et al. Valorization of CO_2 through lithoautotrophic production of sustainable chemicals in *Cupriavidus necator*. *Metab. Eng.* **62**, 207–220 (2020).
49. Green, M. A. et al. Solar cell efficiency tables (version 55). *Prog. Photovoltaics Res. Appl.* **28**, 3–15 (2020).
50. Job, E. *Canadian Solar Sets a 22.80% Conversion Efficiency World Record for P-Type Large Area Multi-crystalline Silicon Solar Cell* (Canadian Solar, 2019); https://investors.canadiansolar.com/news-releases/news-release-details/canadian-solar-sets-2280-conversion-efficiency-world-record-p
51. *North America Land Data Assimilation System (NLDAS) Daily Sunlight (KJ/m²) (1979–2011) Request* (CDC WONDER Online Database, 2013); https://wonder.cdc.gov/NASA-INSOLAR.html
52. Schleusener, M. & Roemer, H. *Illinois Agricultural Statistics 2016 Annual Bulletin*. (USDA, 2016); https://www.nass.usda.gov/Statistics_by_State/Illinois/Publications/Annual_Statistical_Bulletin/2016/2016-IL_Annual_Bulletin_Entire_Report.pdf
53. Clifford, C. B. *Composition of Corn and Yield of Ethanol from Corn* (Penn State Univ., accessed December 10, 2020;) https://www.e-education.psu.edu/egee439/node/672
54. Verduyn, C., Stouthamer, A. H., Scheffers, W. A. & van Dijken, J. P. A theoretical evaluation of growth yields of yeasts. *Antonie Van Leeuwenhoek* **59**, 49–63 (1991).
55. *NIST Chemistry WebBook, SRD 69* (National Institute of Standards and Technology, 2018); https://www.nist.gov/
56. Spieser, H. *Burning Shelled Corn as a Heating Fuel* (Ontario Ministry of Agriculture, Food, and Rural Affairs, 2011); http://www.omafra.gov.on.ca/english/engineer/facts/11-021.htm
57. Zhu, X.-G., Long, S. P. & Ort, D. R. Improving photosynthetic efficiency for greater yield. *Annu. Rev. Plant Biol.* **61**, 235–261 (2010).
58. Mongiovi, P. Heat of combustion of *S. cerevisiae* grown in batch culture on glucose. (*BioNumbers*, accessed December 10, 2020) https://bionumbers.hms.harvard.edu/bionumber.aspx?&id=101698&ver=0
59. *Standard Weight per Bushel for Agricultural Commodities* (Illinois General Assembly, accessed December 10, 2020) https://www.ilga.gov/commission/jcar/admincode/008/00800600ZZ9998bR.html
60. Waskom, M. seaborn.boxplot—seaborn 0.10.1 documentation. Accessed December 10, 2020; https://seaborn.pydata.org/generated/seaborn.boxplot.html

Acknowledgements

We thank J. Kirkwood (University of California, Riverside (UCR)) and the Institute of Integrative Genome Biology Metabolomics Core Facility at UCR for help with metabolomics analysis; the UCR Plant Transformation Research Center, where all plant experiments were conducted; H. Blanch (UCR) for advice on the efficiency calculations; Y. Li (UCR), S. Xu (UCR) and S. Wu (UCR) for advice and reagents for the yeast experiments; J. Hoover (UCR) for his early efforts towards acetate isolation; C. Mendoza (UCR) for help early on with the algae experiments; and M. Jouny (University of Delaware) for his efforts in developing the early concept of the two-step process. We thank T. Xiang (University of North Carolina, Charlotte), B. Velazquez Benitez (UCR), S. Frey (UCR) and J. Russo (UCR) for providing feedback on the manuscript. The following funding supported this work: Translational Research Institute for Space Health (TRISH) through NASA grant no. NNX16AO69A (R.E.J., E.H., M.H.-D., M.L.O.-C. and A.N.), Foundation for Food & Agriculture Research grant no. FF-NIA20–000000009 (R.E.J.), National Science Foundation grant no. DBI-1922642 (M.H.-D.), a Link Foundation Energy Fellowship (E.H.), Department of Energy grant no. DE-FE0029868 (F.J. and S.O.) and National Science Foundation grant no. CBET-1803200 (F.J. and S.O.). The content of this publication is solely the responsibility of the authors and does not necessarily represent the official views of the Foundation for Food & Agriculture Research (FFAR).

Author contributions

R.E.J. and F.J. conceived the experiments. S.O. performed the CO_2 electrolysis experiments. E.C.H. and D.N.L. performed the algae experiments. E.C.H. performed the yeast experiments. R.E.J. performed the mushroom experiments. M.H.-D., A.F.N. and M.L.O.-C. helped conceive the plant experiments, performed them and analysed the data for them. S.O. calculated the efficiencies for electrocatalysis and R.E.J. and E.C.H. calculated the efficiencies for food production. R.E.J., F.J., S.O., E.C.H. and M.H.-D. analysed the data and wrote the manuscript. All authors edited and approved the manuscript.

Competing interests

The authors declare no competing interests.

Additional information

Extended data is available for this paper at https://doi.org/10.1038/s43016-022-00530-x.

Supplementary information The online version contains supplementary material available at https://doi.org/10.1038/s43016-022-00530-x.

Correspondence and requests for materials should be addressed to Feng Jiao or Robert E. Jinkerson.

Peer review information *Nature Food* thanks Daniel Ducat, Jinlong Gong and the other, anonymous, reviewer(s) for their contribution to the peer review of this work.

Reprints and permissions information is available at www.nature.com/reprints.

Publisher's note Springer Nature remains neutral with regard to jurisdictional claims in published maps and institutional affiliations.

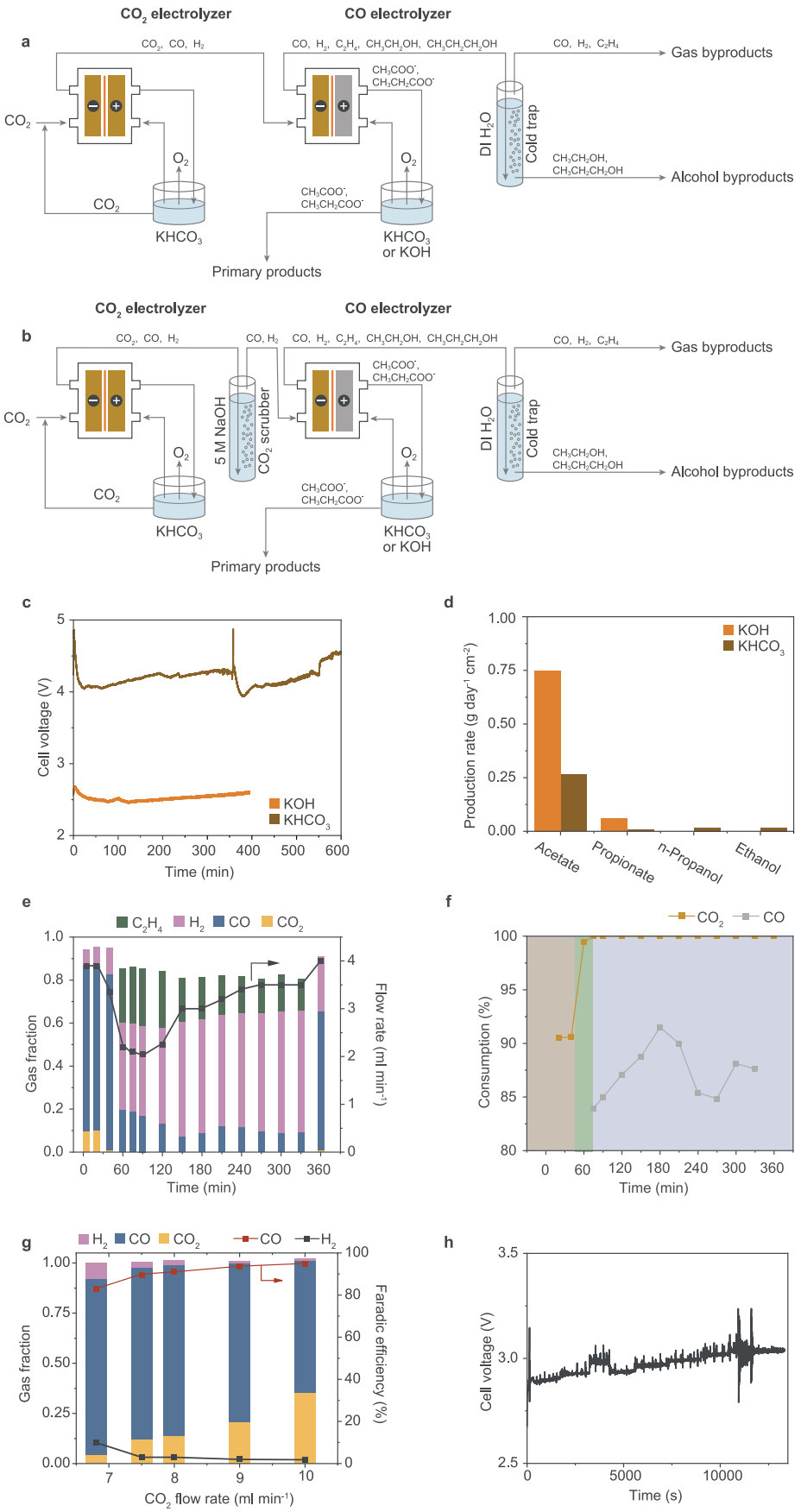

Extended Data Fig. 1 | See next page for caption.

Extended Data Fig. 1 | Tandem CO_2 electrochemical system for the production of acetate. a,b, Schematic of the two-step electrolysis system without (**a**) and with (**b**) 5 M NaOH scrubber. Oxygen was allowed to vent to the atmosphere from anolytes. Primary products were used as effluents for growth. **c**, Electrolyser voltage of direct feed CO electrolyser using 2 M KOH and 1 M $KHCO_3$. 1 M $KHCO_3$ was produced in two separate effluents. Electrolyte was changed at 380 minutes, causing the large spike in potential. 0.476 M acetate: 1 M $KHCO_3$ was produced in the first half of the $KHCO_3$ experiment, 0.648 M acetate: 1 M $KHCO_3$ in the second half, and 0.691 M acetate: 1 M KOH was produced in the 2 M KOH experiment. **d**, Normalized production rate of dissolved CO reduction products collected in the effluent. Liquid product production rate from $KHCO_3$ is cumulative from both experiments, and represents the average over the entire experiment. Data presented represents one experiment for each electrolyte. **e**, Outlet molar fractions of gas products and feeds from the two-step electrolyser system (left axis). Flow rate (right axis) was measured continuously and is indicated by the arrow. The 5 M NaOH scrubber introduced at 30 minutes completely removed CO_2. The CO electrolyser operated from 45 to 345 minutes. The increase in flow rate is attributed to the increase in H_2 production over the course of experiment in the CO_2 electrolyser. **f**, Conversion of CO_2 and CO during the reaction. The CO_2 electrolyser was run without the scrubber at first (grey), a 5 M NaOH scrubber was introduced at 45 minutes (green), the CO electrolyser began operation at 60 minutes (blue). No CO_2 was detected on gas chromatogram after the 5 M NaOH scrubber was introduced. CO conversion is based on the average CO flow rate measured before CO electrolyser operation. **g**, Outlet molar concentrations of gas products and feeds (left axis) for CO_2 electrolyser and corresponding Faradaic efficiencies towards CO and H_2 (right axis) at varied inlet CO_2 flow rates. The arrow indicates the red and black scatter belong to the Faradaic efficiency of the system. **h**, Electrolyser voltage over the course of the flow rate experiment. Oscillations in cell voltage are due to oscillations in the back pressure controller. Step changes were caused by a decrease in inlet CO_2 flow rate.

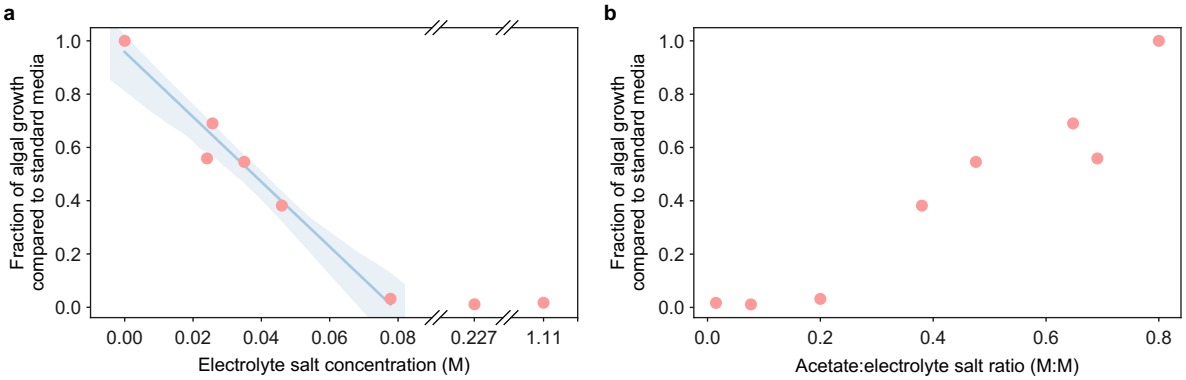

Extended Data Fig. 2 | *Chlamydomonas* growth varies depending on salinity and acetate:electrolyte ratio of media. a, The fraction of growth compared to growth in standard acetate media as electrolyte salt concentrations increased. Fraction of growth was calculated as cells per ml of culture grown in effluent media divided by cells per ml of culture grown in acetate positive control media on the last day of growth. Growth was not observed for electrolyte salt concentrations above 80 mM. Media made with effluents that have lower electrolyte concentrations support higher amounts of growth. Standard acetate media is represented as 0 M. Line is a linear regression ($R^2 = 0.969$). **b**, The same data as in **a** but plotted against acetate: electrolyte salt ratio. Media made with effluents with higher acetate-to-electrolyte salt ratio support higher amounts of growth. The threshold for growth is between 0.2 and 0.4 acetate-to-electrolyte salt ratio. Standard Tris-acetate-phosphate (TAP) media is arbitrarily set to a ratio of 0.8 since it contains no electrolyte. These graphs do not include growth of *Chlamydomonas* with the most optimized effluents, as seen in Fig. 3. *Chlamydomonas* cultures were grown in TAP media with effluent in place of acetate to match the acetate concentration of a typical liquid heterotrophic growth medium (17.5 mM). All media was adjusted to pH 7.2.

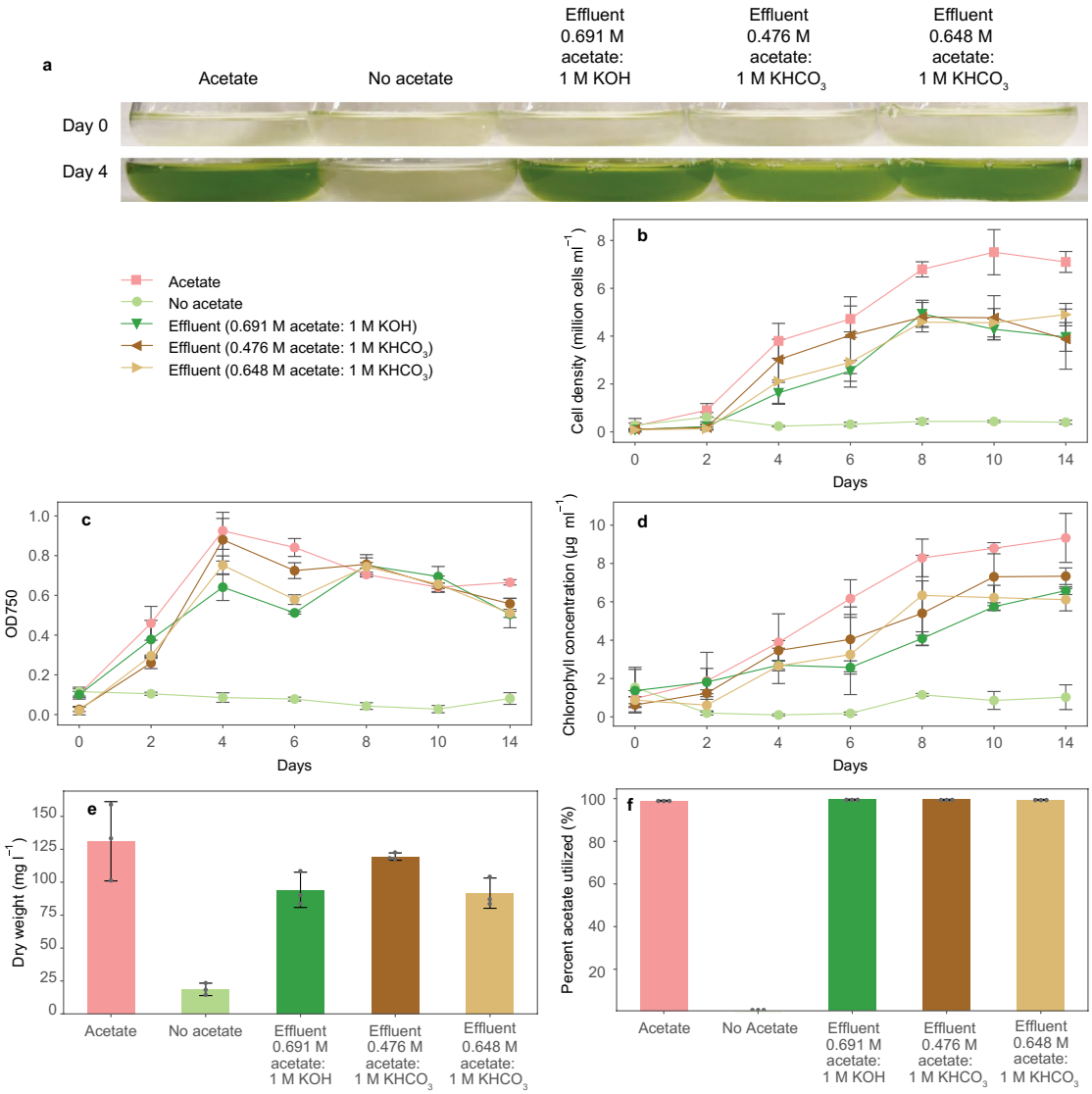

g Mushroom mycelium ability to colonize substrate with varying levels of effluent

	Acetate level from effluent (w/w)				
	0.5%	1.0%	1.5%	2.0%	2.5%
Pearl Oyster	+++	++	+	-	-
Elm Oyster	+++	+	-	-	-
Blue Oyster	++	-	-	-	-
Enokitake	++	-	-	-	-
Coral Tooth	++	-	-	-	-

+++ Full colonization + Limited colonization

++ Partial colonization - No colonization

h Enokitake mushroom mycelium growth with different carbon sources

i Pearl Oyster mushroom mycelium growth with different carbon sources

Extended Data Fig. 3 | See next page for caption.

Extended Data Fig. 3 | *Chlamydomonas* and mushroom mycelium can grow heterotrophically with electrolyser produced effluent as the sole carbon and energy source. a, b, c, d, e, *Chlamydomonas* grown in the dark with electrolyser produced effluents (0.691 M acetate: 1 M KOH, 0.476 M acetate: 1 M $KHCO_3$, and 0.648 M acetate: 1 M $KHCO_3$), acetate, and no acetate. (**a**) Images taken on day 0 and 4, (**b**) cell counts, (**c**) optical density (OD) (750 nm), (**d**) chlorophyll concentration, (**e**) and dry weight after 16 days of growth. **f**, Percentage of acetate in media utilized by *Chlamydomonas* growth determined by comparing NMR measured acetate concentration of media before and after growth. Cultures were grown in Tris-acetate-phosphate (TAP) media with acetate, without acetate (TP), or with effluent in place of acetate to match the acetate concentration of a typical liquid heterotrophic growth medium (17.5 mM). All media was adjusted to pH 7.2. Each data point represents three biological replicates. Error bars indicate standard deviations. Images are representative of all replicates. **g**, Mushroom mycelium's ability to colonize vermiculite substrate soaked with YPD media with no glucose (0 g l^{-1}) and increasing levels of effluent as the carbon source. Full colonization (+++) represents 75% to 100% of substrate colonized, partial colonization (++) represents 15% to 75%, limited colonization (+) represents 1% to 15% of substrate colonized. Effluent added to reach 0.5% (w/w) acetate could support the growth of all fungal species evaluated. **h, i**, Images of pearl oyster (**h**) and enokitake (**i**) mushroom mycelium colonization of a solid vermiculite substrate soaked with YPD media containing glucose (20 g l^{-1}), glucose (20 g l^{-1}) and effluent (0.0691 M acetate: 1 M KOH) added to reach 0.5% (w/w) acetate, or only effluent (0.0691 M acetate: 1 M KOH) in place of glucose (0 g l^{-1}) to reach 0.5% (w/w) acetate as the primary carbon and energy source. Images were taken 24 days post inoculation and are representative of at least 3 replicates. Substrates were fully colonized for all three media. The morphology of the pearl oyster mycelium on top of the effluent containing substrate was different and not as 'fluffy' as compared to the glucose containing media. Images are representative of at least 3 replicates. Scale bars: 20 mm.

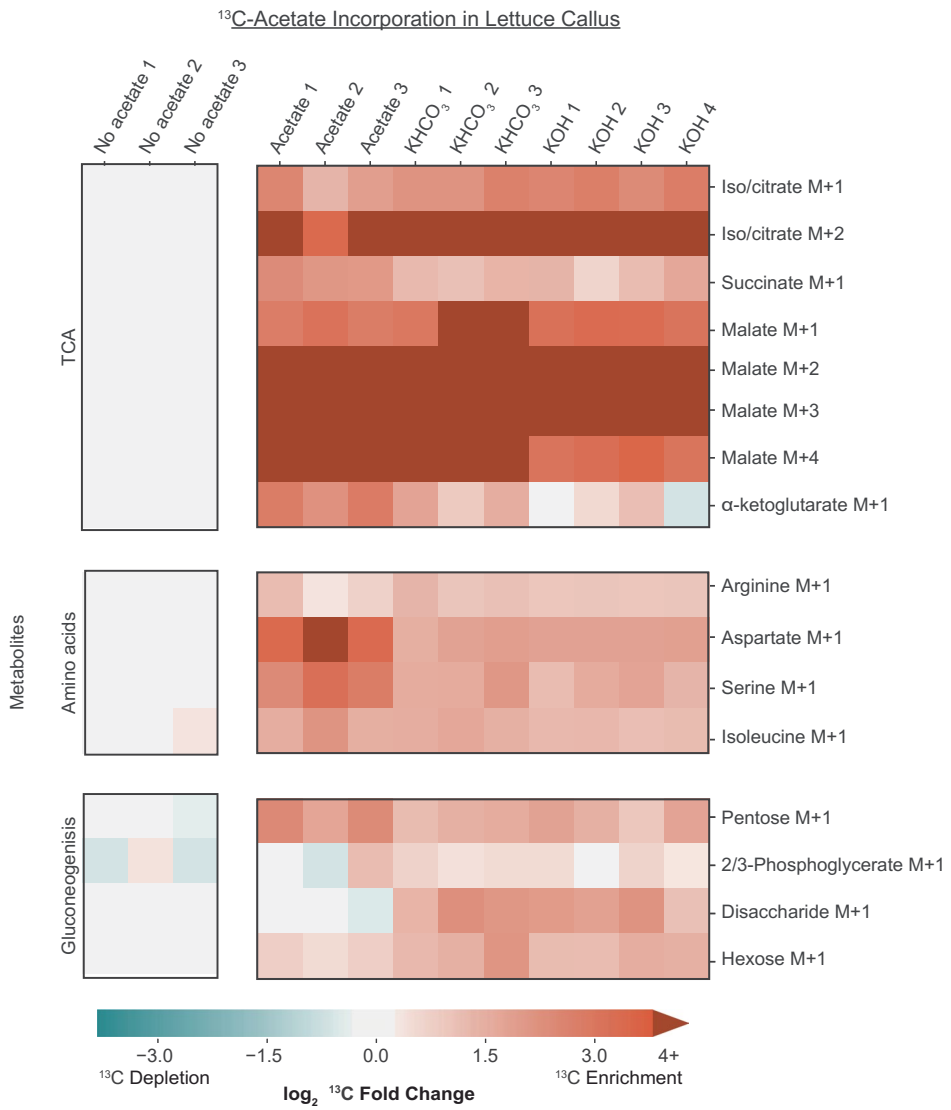

Extended Data Fig. 4 | Heat map of metabolites that had ^{13}C-labeling in undifferentiated lettuce cells (calli). Heat map of all the replicates of the lettuce callus samples treated with no acetate (n = 3), 2 mM ^{13}C-acetate (n = 3), 5 mM ^{13}C-acetate + 5 mM acetate from $KHCO_3$ effluent (0.648 M acetate: 1 M $KHCO_3$, n = 3), or 5 mM ^{13}C-acetate + 5 mM acetate from KOH effluent (0.691 M acetate: 1 M KOH, n = 4). Number after treatment corresponds to the replicate number. Log_2 fold enrichment of ^{13}C between treated and untreated samples, see methods. All samples were grown in the dark showing the ability of plant cells to incorporate ^{13}C from acetate into biomass without light. M+1, 2, 3 or 4 denotes the additional mass of a molecule, which corresponds to the number of carbons in a molecule that are labeled with carbon isotopes.

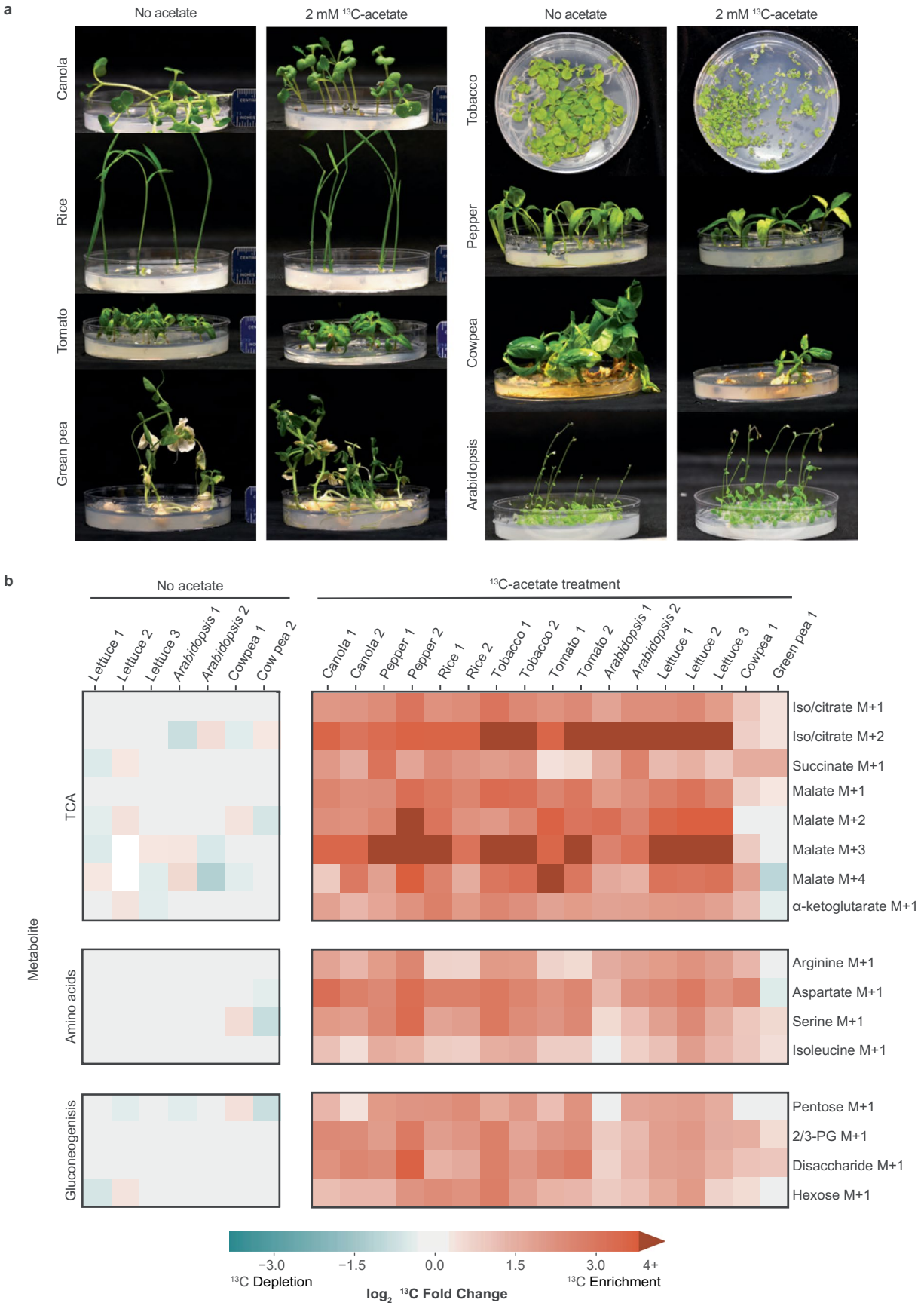

Extended Data Fig. 5 | See next page for caption.

Extended Data Fig. 5 | Heat map of labeled metabolites in crops grown on $^{13}C_2$-acetate. a, Representative images showing crop plants grown with 2 mM ^{13}C-acetate 1/2 MS media and control 1/2 MS media. These plants were later used for metabolomic analysis seen in Fig. 4a. **b**, Heat map of the $\log_2$ enrichment of ^{13}C-labeling in all crop replicates compared to the average value of non-treated controls used to create Fig. 4a. The number after each plant name at the top of the figure corresponds to the replicate number. Samples grown without acetate with only one replicate are not included. There is enrichment in all treated crop samples. There are lower levels of ^{13}C-enrichment in green pea relative to other crops. This may be due to a larger reliance for carbon and energy from the endosperm of the seed resulting in less absorption of nutrients and $^{13}C_2$-acetate from the growth media.

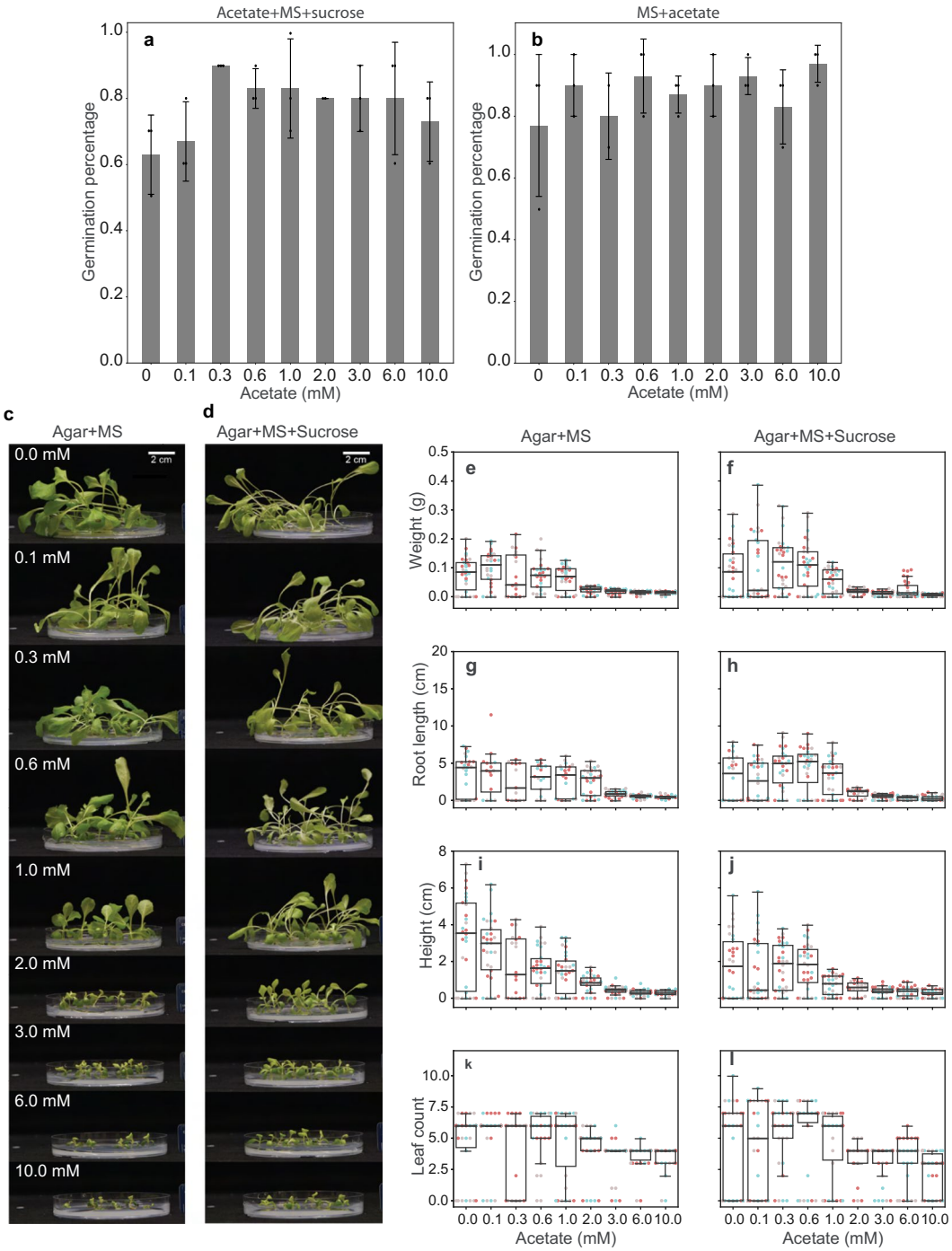

Extended Data Fig. 6 | Effect of increasing levels of acetate exposure on lettuce germination and growth (0.0, 0.1, 0.3, 0.6, 1.0, 2.0, 3.0, 6.0, 10 mM). **a, b**, Seed germination rate for lettuce after 28 days on (**a**) agar + 1/2 MS + sucrose + acetate (**b**) agar + 1/2 MS + acetate. 1/2 MS is a typical plant nutrient mix for growth on agar. Seed germination percent is not significantly different from controls across all treatments (Tukey's HSD all p-values >0.15). All error bars represent the standard deviation between the germination percentage of the replicates (3 biological replicates with 10 seeds each). Images of lettuce seed germination and growth. **c, d**, The media was made of (**c**) 1/2 MS + acetate, and (**d**) 1/2 MS + sucrose + acetate. (**c**) 1/2 MS + acetate visually shows the effect of acetate on plant growth in a concentration dependent manner. (**d**) Agar + 1/2 MS + sucrose + acetate shows that supplementing lettuce with an additional carbon source, sucrose, does not affect the concentration dependent inhibition. All images are representative of all biological replicates for each treatment (3 biological replicates with 10 seeds each). **e-l** Quantify plant growth measurements: weight, root length, stem height, and leaf count for lettuce plants (~30 individuals shown, and 3 biological replicates visualized in red, grey, and blue for each treatment). **e, g, i** and **k**, show agar + 1/2 MS + acetate. There is an acetate concentration dependent inhibition of plant growth that occurs at different concentrations of acetate for different traits, height being the most sensitive and leaf count being the least sensitive. **f, h, j** and **l**, show agar + 1/2 MS + sucrose + acetate. Again, there is inhibition of growth at higher acetate concentrations of acetate (2-10 mM). It did not appear that the addition of sucrose had a strong effect on growth, positive or negative, in combination with acetate. The box plots encompasses the quartiles of the dataset and the whiskers capture the rest of the data distribution, except for points that are determined to be "outliers" based on a function of the interquartile range[60].

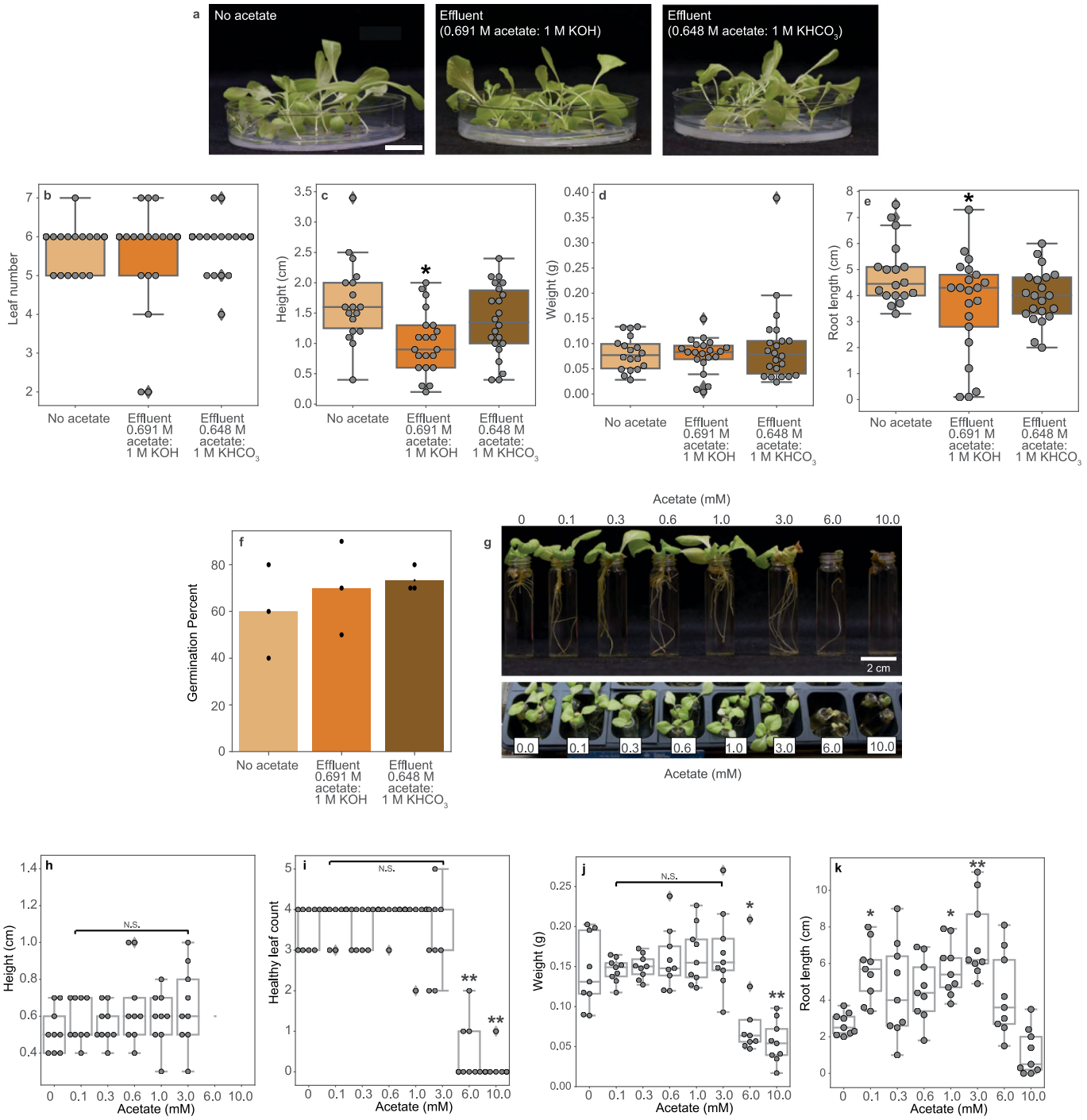

Extended Data Fig. 7 | See next page for caption.

Extended Data Fig. 7 | Lettuce plants grown on electrolysis effluent and liquid media with acetate feeding. a, Representative images of lettuce seeds that were germinated and grown on control 1/2 MS no acetate media, 1/2 MS media supplemented with 1 mM acetate KOH effluent (0.691 M acetate: 1 M KOH), and 1/2 MS media supplemented with 1 mM acetate Bicarbonate effluent (0.648 M acetate: 1 M $KHCO_3$) (3 biological replicates with 10 seeds each with at least 18 total seeds germinating in each treatment). White scale bar is 2 cm. All treatments had 3 biological replicates with 10 seeds each that were grown for 28 days and then growth parameters were measured and photographed. The white scale bar represents 2 cm. **b, c, d, e** and **f**, show the leaf number, height, fresh weight, root length, and germination rate, respectively, of lettuce plants germinated and grown on no acetate, 1 mM acetate KOH effluent (0.691 M acetate: 1 M KOH), and 1 mM acetate bicarbonate effluent (0.648 M acetate: 1 M $KHCO_3$). There was no statistical difference in weight between lettuce grown with ($n = 21$) and without ($n = 18$) effluent (p-value >0.05, Tukey's HSD). However there was a significant difference between the 0.691 M acetate: 1 M KOH for root length and height, which could suggest that the potassium salt may cause some level of inhibition. **g**, Representative images of the acetate feeding experiment performed on lettuce seedling. Lettuce seedlings were germinated for 11 days and then cut at the base of the stem and transferred to water and acetate solutions at acetate concentrations of 0, 0.1, 0.3, 0.6, 1, 3, 6 and 10 mM ($n = 9$ biological replicates for each treatment). **h, i, j** and **k**, show the height, leaf count, length of the roots, and the weight of the plants respectively. Root length was significantly increased in the presence of acetate (p-value <0.001, Tukey's HSD) ($n = 9$ for each treatment). Height for 6 and 10 mM is not included due to incompatibility with the method of measuring the height, which was the distance from the top of the stem to the first lateral root, at these higher levels of acetate concentration there was poor root development, which led to artificially inflated height. There is a significant increase in root length in lower levels of acetate concentration (0.1, 1, and 3 mM) based on Tukey's HSD statistical test, before higher acetate levels start to inhibit root growth. Significant p-values from Tukey's HSD comparing controls to treatment are denoted by an asterisk, p-value <0.05, double asterisk is a p-value <0.001, N.S. denotes no significant difference from controls (p-value > 0.05). All box plots encompass the quartiles of the dataset and the whiskers capture the rest of the data distribution, except for points that are determined to be "outliers" based on a function of the interquartile range[60].

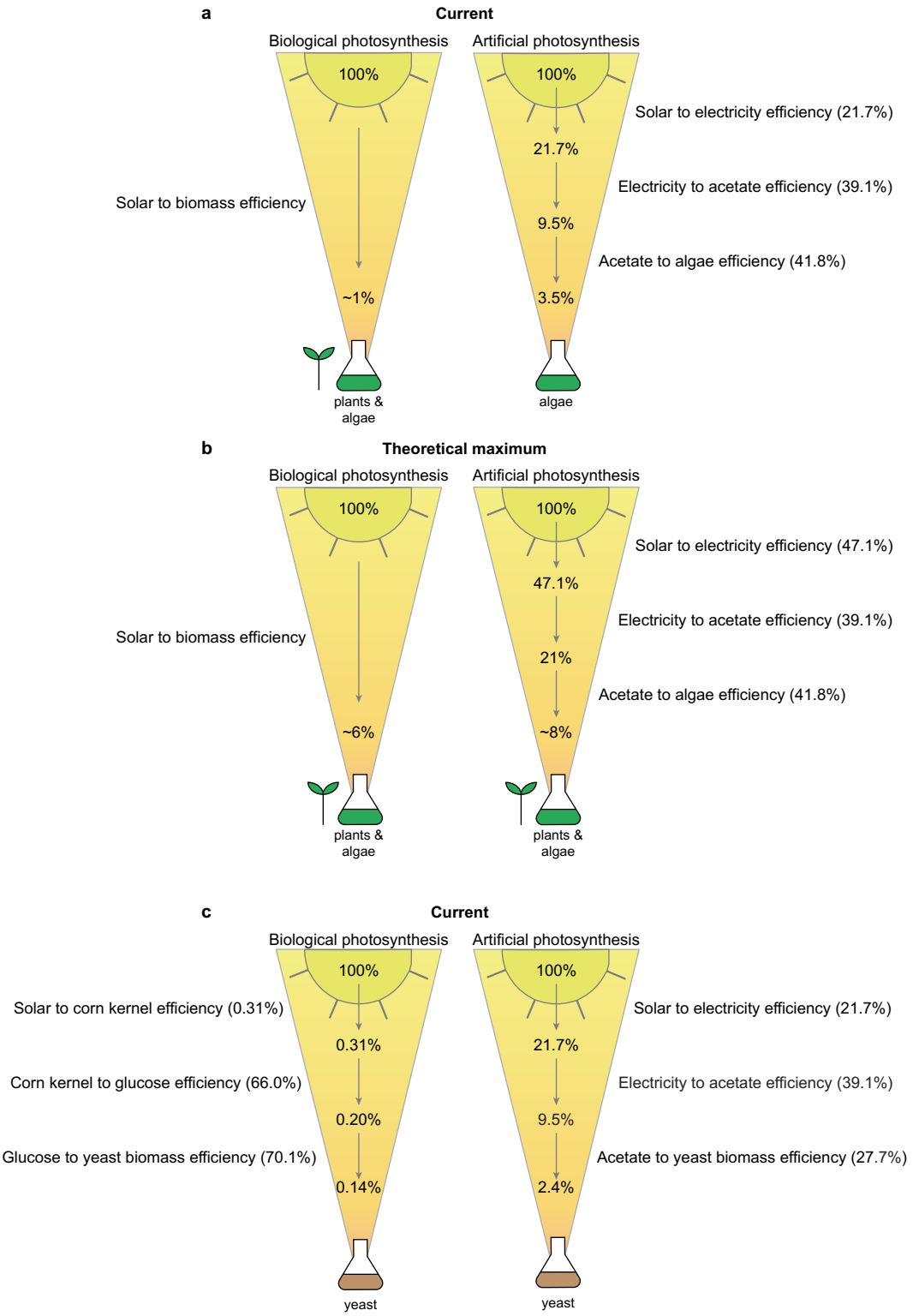

Extended Data Fig. 8 | See next page for caption.

Extended Data Fig. 8 | Energy efficiency of food production from artificial photosynthesis compared to biological photosynthesis. The energy efficiency of sunlight to food production through artificial photosynthesis and biological photosynthesis are compared. Major steps in energy conversion from sunlight (100% solar energy) to food are represented by arrows, with the percentage of remaining energy after each step indicated. The energy efficiency of each step is noted in parentheses. **a**, Same data as in Fig. 5. The current efficiency numbers for algae production through artificial photosynthesis were determined in this work through experimentation (electricity to acetate and acetate to algae efficiencies). The value for solar to electricity efficiency is based on a commercially available silicon solar cell[49,50]. The value for biological photosynthetic efficiency was obtained from the literature[1]. **b**, Theoretical maximum efficiencies for both biological photosynthesis and artificial photosynthesis are given to show the potential of these approaches. The theoretical maximum efficiency for biological photosynthesis (6%) is for C4 plants (including maize, sugarcane, and sorghum). The theoretical maximum efficiency of biological photosynthesis for C3 plants (including rice, tomato, pepper, and cowpea) is 4.6% (not shown)[57]. The value for solar to electricity efficiency (47.1%) is from a lab demonstration of a multi-junction solar cell under concentrated illumination[49]. Continued improvements to electrolysis technology and acetate utilization in plants and algae would increase the overall efficiency of this artificial photosynthetic approach. **c**, The current efficiency numbers for nutritional yeast production through artificial photosynthesis were determined in this work through experimentation (electricity to acetate and acetate to yeast efficiencies). The value for solar to electricity efficiency is based on a commercially available silicon solar cell[49,50]. Nutritional yeast is typically grown using glucose derived from plants, such as corn. The efficiency was calculated using values for solar irradiance and corn productivity in Illinois, USA[51,52].

nature portfolio

Corresponding author(s): Robert Jinkerson

Last updated by author(s): May 4, 2022

Reporting Summary

Nature Portfolio wishes to improve the reproducibility of the work that we publish. This form provides structure for consistency and transparency in reporting. For further information on Nature Portfolio policies, see our Editorial Policies and the Editorial Policy Checklist.

Statistics

For all statistical analyses, confirm that the following items are present in the figure legend, table legend, main text, or Methods section.

n/a	Confirmed	
☐	☒	The exact sample size (*n*) for each experimental group/condition, given as a discrete number and unit of measurement
☐	☒	A statement on whether measurements were taken from distinct samples or whether the same sample was measured repeatedly
☐	☒	The statistical test(s) used AND whether they are one- or two-sided *Only common tests should be described solely by name; describe more complex techniques in the Methods section.*
☒	☐	A description of all covariates tested
☒	☐	A description of any assumptions or corrections, such as tests of normality and adjustment for multiple comparisons
☐	☒	A full description of the statistical parameters including central tendency (e.g. means) or other basic estimates (e.g. regression coefficient) AND variation (e.g. standard deviation) or associated estimates of uncertainty (e.g. confidence intervals)
☐	☒	For null hypothesis testing, the test statistic (e.g. *F*, *t*, *r*) with confidence intervals, effect sizes, degrees of freedom and *P* value noted *Give P values as exact values whenever suitable.*
☒	☐	For Bayesian analysis, information on the choice of priors and Markov chain Monte Carlo settings
☒	☐	For hierarchical and complex designs, identification of the appropriate level for tests and full reporting of outcomes
☒	☐	Estimates of effect sizes (e.g. Cohen's *d*, Pearson's *r*), indicating how they were calculated

Our web collection on statistics for biologists contains articles on many of the points above.

Software and code

Policy information about availability of computer code

Data collection	No software was used for data collection for this study.
Data analysis	Statistics were calculated with Python (2.7.11), SciPy (0.17.0), Pandas (0.18.1), and statsmodels.

For manuscripts utilizing custom algorithms or software that are central to the research but not yet described in published literature, software must be made available to editors and reviewers. We strongly encourage code deposition in a community repository (e.g. GitHub). See the Nature Portfolio guidelines for submitting code & software for further information.

Data

Policy information about availability of data

All manuscripts must include a data availability statement. This statement should provide the following information, where applicable:

- Accession codes, unique identifiers, or web links for publicly available datasets
- A description of any restrictions on data availability
- For clinical datasets or third party data, please ensure that the statement adheres to our policy

Metabolomics data (Fig. 4a, Extended Data Figs. 4 and 5b) and all source data can be found at https://doi.org/10.6086/D1VT2V in the Dryad Digital Repository.

Field-specific reporting

Please select the one below that is the best fit for your research. If you are not sure, read the appropriate sections before making your selection.

☒ Life sciences ☐ Behavioural & social sciences ☐ Ecological, evolutionary & environmental sciences

For a reference copy of the document with all sections, see nature.com/documents/nr-reporting-summary-flat.pdf

Life sciences study design

All studies must disclose on these points even when the disclosure is negative.

Sample size	Sample sizes were chosen based on similar experiments previously reported in the literature.
Data exclusions	Only one sample (Bicarb_Callus_(5mM_C13_48_hr)-1) was excluded from the analysis because it was marked as an outlier by the Dixon Q test when compared to the other 3 replicates. It showed extremely high levels of C13 incorporation but at levels that were not consistent with other replicates and when included in our analysis it would skew our results (such as the average) showing higher levels of C13 incorporation than was consistently achieved.
Replication	Trial runs were preformed to establish our methods and then full experiments with multiple replicates showed consistent and repeatable results.
Randomization	Plant seeds, algae, and fungi were all randomly divided into separate experimental groups for testing specific treatments.
Blinding	There was no blinding but methods of measurement were established and consistent across all samples in addition to inherently unbiased sample measurements by instruments (LC-MS, scales, cell counter etc).

Reporting for specific materials, systems and methods

We require information from authors about some types of materials, experimental systems and methods used in many studies. Here, indicate whether each material, system or method listed is relevant to your study. If you are not sure if a list item applies to your research, read the appropriate section before selecting a response.

Materials & experimental systems

n/a	Involved in the study
☒	☐ Antibodies
☐	☒ Eukaryotic cell lines
☒	☐ Palaeontology and archaeology
☒	☐ Animals and other organisms
☒	☐ Human research participants
☒	☐ Clinical data
☒	☐ Dual use research of concern

Methods

n/a	Involved in the study
☒	☐ ChIP-seq
☒	☐ Flow cytometry
☒	☐ MRI-based neuroimaging

Eukaryotic cell lines

Policy information about cell lines

Cell line source(s)	Chlamydomonas Resource Center
Authentication	No cell lines used were authenticated
Mycoplasma contamination	Cell lines were not tested for mycoplasma contamination
Commonly misidentified lines (See ICLAC register)	No commonly misidentified lines were used in this study